

New Serotonin 5-HT_{1A} Receptor Agonists with Neuroprotective Effect against Ischemic Cell Damage

Isabel Marco,^{†,‡} Margarita Valhondo,^{†,‡} Mar Martín-Fontecha,[†] Henar Vázquez-Villa,[†] Joaquín Del Río,[‡] Anna Planas,[§] Onintza Sagredo,^{||} José A. Ramos,^{||} Iván R. Torrecillas,[⊥] Leonardo Pardo,[⊥] Diana Frechilla,[‡] Bellinda Benhamú,^{*,†} and María L. López-Rodríguez^{*,†}

[†]Departamento de Química Orgánica I, Facultad de Ciencias Químicas, Universidad Complutense de Madrid, E-28040 Madrid, Spain

[‡]Area de Neurociencias, CIMA, Universidad de Navarra, E-31008 Pamplona, Spain

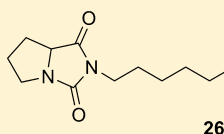
[§]Institut d'Investigacions Biomèdiques, CSIC, IDIBAPS, E-08036 Barcelona, Spain

^{||}Departamento de Bioquímica y Biología Molecular, Facultad de Medicina, Universidad Complutense de Madrid, E-28040 Madrid, Spain

[⊥]Laboratori de Medicina Computacional, Unitat de Bioestadística, Facultat de Medicina, Universitat Autònoma de Barcelona, E-08913 Bellaterra, Barcelona, Spain

Supporting Information

ABSTRACT: We report the synthesis of new compounds 4–35 based on structural modifications of different moieties of previously described lead UCM-2550. The new nonpiperazine derivatives, representing second-generation agonists, were assessed for binding affinity, selectivity, and functional activity at the 5-HT_{1A} receptor (5-HT_{1A}R). Computational β_2 -based homology models of the ligand–receptor complexes were used to explain the observed structure–affinity relationships. Selected candidates were also evaluated for their potential in vitro and in vivo neuroprotective properties. Interestingly, compound 26 (2-{6-[(3,4-dihydro-2H-chromen-2-ylmethyl)amino]hexyl}-tetrahydro-1H-pyrrolo[1,2-c]imidazole-1,3(2H)-dione) has been characterized as a high-affinity and potent 5-HT_{1A}R agonist ($K_i = 5.9$ nM, $EC_{50} = 21.8$ nM) and exhibits neuroprotective effect in neurotoxicity assays in primary cell cultures from rat hippocampus and in the MCAO model of focal cerebral ischemia in rats.



$K_i = 5.9$ nM
 $EC_{50} = 21.8$ nM
MCAO: 29% reduction of cerebral infarct volume

INTRODUCTION

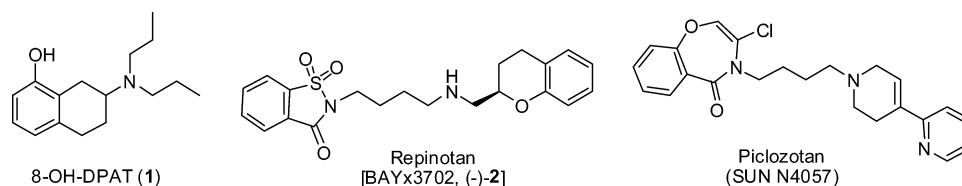
G protein-coupled receptors (GPCRs) are the largest family of membrane-bound receptors and transmit chemical signals into a wide array of different cell types. These proteins account for more than the 50% of the druggable genome and present a wide range of opportunities as therapeutic targets in areas including cancer, cardiac dysfunction, diabetes, central nervous system disorders, obesity, inflammation, and pain.¹ Indeed, drugs targeting members of this integral membrane protein superfamily represent the core of modern medicine because they account for the majority of best-selling drugs and about 40% of all prescription pharmaceuticals on the market. Nevertheless, there is still much to be learned about how GPCRs work and how they can be selectively modulated. Technologies designed specifically to tackle the GPCR challenge, such as cell-based screening assays and structural studies, are blossoming and reinforcing their potential for future drug discovery.^{2–4} Consequently, GPCRs are among the most heavily investigated drug targets, and there is broad consensus that they will remain at the hub of drug development activities for the foreseeable future.

Serotonin (5-hydroxytryptamine, 5-HT) receptors constitute an important GPCR family composed of 14 members which have been classified into seven families (5-HT_{1–7}) based on amino acid sequences, pharmacology, and intracellular

mechanisms.^{5,6} The 5-HT_{1A} receptor (5-HT_{1A}R) subtype has been the most extensively studied, its agonists and partial agonists being clinically used in the treatment of anxiety and depression.^{7–9} The 5-HT_{1A}R is also responsible for the lack of unwanted side-effects in some atypical antipsychotic drugs.^{10,11} Besides these well-established therapeutic areas, other interesting nonpsychiatric perspectives have emerged for 5-HT_{1A}R agents in recent years, mostly related to neuroprotection, cognitive impairment, Parkinson's disease, or pain treatment.^{12–15} In particular, it is known that the selective 5-HT_{1A}R agonist 8-hydroxy-2-(di-*n*-propylamino)tetrinalin (8-OH-DPAT, **1**) and other 5-HT_{1A}R agonists attenuate excitotoxicity (Chart 1),¹⁶ showing neuroprotective properties in models of global and focal cerebral ischemia in mice, rats, and gerbils.^{17,18} Indeed, the selective 5-HT_{1A}R agonists repinotan [(*R*)-(-)-2-{4-[(chroman-2-ylmethyl)amino]butyl}-1,1-dioxobenzo[*d*]isothiazolone (BAYx3702, (-)-**2**)] and piclozotan (SUN N4057) have demonstrated neuroprotective properties in phase IIb clinical trials for treatment of ischemic stroke, although the former has been discontinued.^{19–21} Stroke is the third leading cause of death in adults and the main neurologic cause of disability in the elderly. It is recognized that cell death

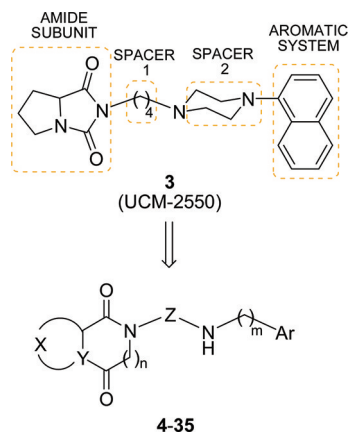
Received: June 17, 2011

Published: October 27, 2011

Chart 1. Structures of 5-HT_{1A}R Agonists Endowed with Neuroprotective Properties

in the ischemic penumbra may be prevented by different classes of compounds acting at different steps along the ischemic cascade. Yet, pharmacological treatment with available so-called neuroprotective drugs has not been successful to improve clinical outcome in patients. Today, several studies strongly support the potential interest of 5-HT_{1A}R activation in the search for neuroprotective strategies.^{22–24} Because stroke is such an important cause of mortality worldwide, even small clinical benefits may have a huge positive impact on public health. In this context, our goal is the development of a 5-HT_{1A}R agonist as an anti-ischemic agent.

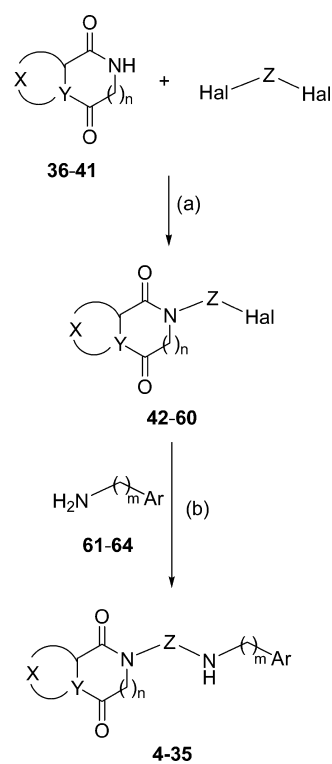
During the last years, our group has been involved in a wide research program aimed at developing new arylpiperazines with high affinity for the 5-HT_{1A}R.^{25–31} Some of these ligands have been pharmacologically characterized as potent 5-HT_{1A}R agonists endowed with anxiolytic properties.^{32,33} In the present work, the previously reported high-affinity ligand **3** (UCM-2550)³¹ was used as starting point to design and synthesize new compounds **4–35** devoid of piperazine ring (Tables 1–4). In these series, we have systematically modified different structural moieties of lead compound **3**: the amide subunit, spacer 1, spacer 2, and the aromatic system (Chart 2). The new

Chart 2. Designed Non-Piperazine Compounds **4–35** Based on High-Affinity 5-HT_{1A}R Ligand **3**

synthesized nonpiperazine ligands **4–35**, representing second-generation 5-HT_{1A}R agonists, were assessed for binding affinity, selectivity, and functional activity at the receptor. The mode of binding proposed in our computational model of ligand–receptor complex explained the observed structure–affinity relationships. Selected candidates have also been evaluated for their potential *in vitro* and *in vivo* neuroprotective properties. In particular, compound **26** [$X = (\text{CH}_2)_3$, $Y = \text{N}$, $n = 0$, $Z = (\text{CH}_2)_6$, $m = 1$, $\text{Ar} = \text{chroman-2-yl}$] was characterized as a potent 5-HT_{1A}R agonist and exhibited neuroprotective effect in neurotoxicity assays in primary cell cultures from rat hippocampus and in a model of focal cerebral ischemia in rats.

RESULTS AND DISCUSSION

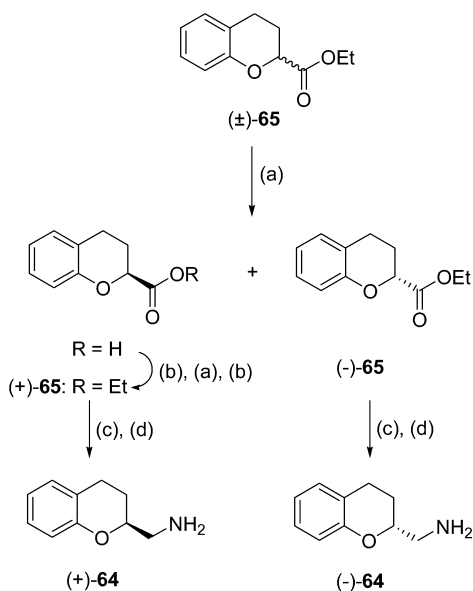
Synthesis. Target compounds **4–35** (Tables 1–4) were obtained following the synthetic route described in Scheme 1.

Scheme 1. Synthesis of Target Compounds **4–35**^a

^aReagents and conditions: (a) NaH, DMF, 110 °C, 40–74%; (b) CH₃CN, 60 °C, 35–58%.

In general, 1,3-thiazolidine-2,4-dione, hydantoin^{34–36} **36–39** [$n = 0$; $Y = \text{N}$; $X = (\text{CH}_2)_3$, $(\text{CH}_2)_4$, CH_2SCH_2 , and $\text{S}(\text{CH}_2)_2$, respectively] or diketopiperazines³⁷ **40,41** [$n = 1$; $Y = \text{N}$; $X = (\text{CH}_2)_3$, and $(\text{CH}_2)_4$, respectively] were alkylated with the appropriate commercially available α,ω -dibromo or -dichloro derivative in the presence of sodium hydride and *N,N*-dimethylformamide (DMF) to yield the corresponding halogenated intermediates **42–60**. Subsequent treatment of **42–60** with commercial or previously described amines^{38–40} **61–64** provided final compounds **4–35**. Enantiopure amines (+)- and (–)-**64** were prepared following a new procedure based on the kinetic resolution of racemic ethyl chromane-2-carboxylate [(±)-**65**]⁴¹ with *Pseudomonas fluorescens* lipase,⁴² followed by further conversion of enantiopure esters (+)- and (–)-**65** into the corresponding amides and subsequent diborane reduction (Scheme 2).

Binding Affinities. New synthesized compounds **4–35** were assessed for *in vitro* affinity at serotonin 5-HT_{1A} receptors by competition binding assays, using [³H]-8-OH-DPAT as

Scheme 2. Synthesis of Enantiopure Amines (+)- and (-)-64^a

^aReagents and conditions: (a) lipase P-30, THF/H₂O, rt, 42% for (–)-65; (b) EtOH, H₂SO₄, reflux, 38% from (±)-65; (c) 28% aq NH₃, NH₄Cl, 100 °C, 70–72%; (d) (BH₃)₂, THF, 0 °C to reflux, 82–86%.

radioligand (see Experimental Section for details). All compounds were assayed as hydrochloride salts. The competitive inhibition assays were first performed at a fixed dose of 10^{−6} M, and the complete dose–response curve, at six different concentrations of the ligand, was determined for those compounds that presented a displacement of the radioligand over 55%. The inhibition constant K_i was calculated from the IC₅₀ value using the Cheng–Prusoff equation,⁴³ and the values in Tables 1–4 are the mean of two to four independent experiments. Compounds exhibiting high affinity for the 5-HT_{1A}R ($K_i < 50$ nM) were tested for selectivity over other serotonin receptors as well as α_1 -adrenergic and dopamine D₂ receptors (Tables 2–4), using the following specific radioligands: 5-HT_{2A}, [³H]ketanserin; 5-HT₃, [³H]LY 278584; 5-HT₄, [³H]GR 113808; 5-HT₇, [³H]-5-CT; α_1 , [³H]prazosin; and D₂, [³H]spiperone (see Experimental Section for details).

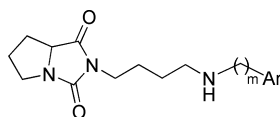
Tables 1–4 show the binding affinities of compounds 4–17, 18–23, and 24–35 obtained from the systematic modification of the different moieties present in the molecule: the amide subunit, spacer 1 (Z), spacer 2 [(CH₂)_m] and the aromatic (Ar) system (Chart 2). The following structure–affinity relationships can be drawn for each series. Clearly, only bicyclic Ar systems are favorable for 5-HT_{1A}R affinity [$K_i(5–9) = 1.23–49$ nM], with the exception of compound 4 [$K_i(4) > 1000$ nM], whereas all derivatives containing a single ring are inactive [$K_i(10–17) > 1000$ nM] (Table 1). Notably, analogue 9—containing a single methylene unit as spacer 2 and chromane as Ar—is the most potent compound. No significant differences were observed between racemic compound (±)-9 ($K_i = 1.23$ nM) and the most active isomer (–)-9 ($K_i = 1.9$ nM). Thus, the (±)-chroman-2-ylmethyl group appeared as the most promising for the Ar and spacer 2 moieties. Using this terminal group, the influence of the amide subunit was studied in compounds 18–23 (Table 3). Modifications in the amide subunit do not have a significant influence because all compounds in the series exhibit high to very high 5-HT_{1A}R

Table 1. 5-HT_{1A}R Affinity of New Synthesized Compounds 4–17

compd	m	Ar	$K_i \pm \text{SEM}$ (nM) ^a
4	1		>1000
5	2		28 ± 3
6	1		49.0 ± 0.5
7	2		43 ± 4
8	1		8.3 ± 0.2
(±)-9	1		1.23 ± 0.09
(–)-9	1		1.9 ± 0.1
(+)-9	1		36.7 ± 0.4
10	1		>1000
11	2		>1000
12	1		>1000
13	2		>1000
14	1		>1000
15	2		>1000
16	1		>1000
17	2		>1000

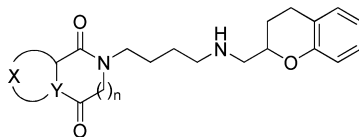
^aValues are the mean of two to four experiments performed in triplicate.

binding affinity [$K_i(18–23) = 2.4–34$ nM]. Considering both affinity data and synthetic availability, 1,3-dioxoperhydropyrrolo[1,2-*c*]imidazole and 1,3-thiazolidine-2,4-dione were selected as the amide subunits in compounds 24–35 for further optimization of spacer 1. In this series, the best results were obtained for compounds with saturated aliphatic spacers containing 3–6 methylene units ($K_i = 1.23–12.9$ nM) (Table 4). The influence of the *cis* (29)/*trans* (28) configuration of the four-methylene spacer was also assessed, the *trans* isomer being more potent [$K_i(28) = 27$ nM vs $K_i(29) = 114$ nM]. Compound 30, containing a triple bond, is inactive. Substitution of methylene units by a phenyl ring is tolerated [$K_i(31) = 28$ nM; $K_i(32) = 42$ nM]. In general, the new synthesized compounds were inactive or poorly active at other 5-HT receptor subtypes as well as dopamine D₂ receptor (Tables 2–4).

Table 2. Selectivity of New 5-HT_{1A}R Ligands 5–9

compd	m	Ar	$K_i \pm \text{SEM (nM)}^a$						
			5-HT _{1A}	5-HT _{2A}	5-HT ₃	5-HT ₄	5-HT ₇	D ₂	α_1
5	2		28 ± 3	>1000	>1000	>1000	>1000	>1000	>1000
6	1		49.0 ± 0.5	>1000	>1000	572 ± 78	8.0 ± 0.9	>1000	>1000
7	2		43 ± 4	157.3 ± 0.7	>1000	594 ± 44	74 ± 7	>1000	99 ± 14
8	1		8.3 ± 0.2	>1000	>1000	>1000	>1000	>1000	>1000
(±)-9	1		1.23 ± 0.09	>1000	>1000	>1000	299 ± 8	>1000	121 ± 2
(-)-9	1		1.9 ± 0.1	>1000	>1000	>1000	41 ± 4	>1000	7.4 ± 0.8
(+)-9	1		36.7 ± 0.4	>1000	>1000	>1000	68 ± 12	>1000	69 ± 16

^aValues are the mean of two to four experiments performed in triplicate.

Table 3. 5-HT_{1A}R Affinity and Selectivity of New Synthesized Compounds 18–23

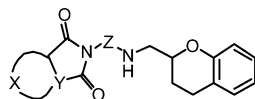
compd	X	Y	n	$K_i \pm \text{SEM (nM)}^a$						
				5-HT _{1A}	5-HT _{2A}	5-HT ₃	5-HT ₄	5-HT ₇	D ₂	α_1
(±)-9		N	0	1.23 ± 0.09	>1000	>1000	>1000	299 ± 8	>1000	121 ± 2
18		N	0	2.4 ± 0.4	>1000	>1000	>1000	66 ± 1	>1000	62 ± 4
19		N	1	21 ± 3	>1000	>1000	>1000	418 ± 52	>1000	107 ± 10
20		N	1	34 ± 1	>1000	>1000	>1000	>1000	>1000	67 ± 11
21		N	0	20 ± 6	>1000	>1000	>1000	493 ± 1	>1000	50 ± 6
22		N	0	13 ± 1	>1000	>1000	>1000	>1000	>1000	8.5 ± 0.6
23	--	S	0	15.1 ± 0.6	>1000	>1000	>1000	169 ± 18	>1000	>1000

^aValues are the mean of two to four experiments performed in triplicate.

Computational Model of 5-HT_{1A}R in Complex with Ligand 26. To date, within the biogenic amine family of GPCRs, the crystal structures of the β_1 -adrenergic receptor bound to the antagonist cyanopindolol (Protein Data Bank accession number 2VT4),⁴⁴ partial agonists dobutamine (2Y01) or salbutamol (2Y04), or agonists carmoterol (2Y02) or isoprenaline (2Y03),⁴⁵ the β_2 -adrenergic receptor bound to the partial inverse agonist carazolol (2RH1),⁴⁶ the agonist BI-167107 (3P0G),⁴⁷ or the irreversible agonist FAUC50 (3PDS),⁴⁸ the dopamine D₃ receptor in complex with the antagonist eticlopride (3PBL),⁴⁹ and the histamine H₁ receptor in complex with doxepin,⁵⁰ have been reported. In adrenergic receptors, all type of compounds (i.e., agonists, partial agonists, antagonists, or inverse agonists) anchor the receptor through a complex hydrogen bond network involving the secondary protonated amine (NH₂⁺) and the β -OH of the ligand and Asp^{3.32} and Asn^{7.39} of the receptor. In contrast, the tertiary protonated amine (NH⁺) of eticlopride or doxepin interacts exclusively with Asp^{3.32} of the dopamine D₃ or histamine H₁ receptor, respectively, due to the presence of a single N–H

bond in the ligand and the absence of Asn^{7.39} in the receptor (Figure 1A). The fact that the Asp^{3.32} and Asn^{7.39} combination of side chains is also present in the 5-HT_{1A}R (Figure 1A) led us to propose a similar hydrogen bond network as in adrenergic receptors. The model depicted in Figure 1B shows the secondary protonated amine (NH₂⁺) and the oxygen atom of the chromane system of **26** anchored between Asp^{3.32} and Asn^{7.39}, the Ar moiety expanded toward transmembrane helix (TM) 5, and the amide subunit extended toward TM 2. Thus, compound **26** occupies the orthosteric binding pocket that is located between the extracellular segments of TMs 3 and 5–7, and the recently named minor binding pocket located between the extracellular segments of TMs 2, 3, and 7.⁵¹ The binding of **26** to the 5-HT_{1A}R resembles the binding of FAUC50 covalently bound to the His^{2.64}Cys mutant β_2 -adrenergic receptor through a disulfide bond.⁴⁸

This mode of binding of **26** explains the observed structure–affinity relationships. (i) The length of spacer 1 can be extended to eight methylene units without a large decrease in binding affinity. Increase of the number of methylene units

Table 4. 5-HT_{1A}R Affinity and Selectivity of New Synthesized Compounds 24–35

Compd	X	Y	Z	$K_i \pm \text{SEM (nM)}^a$						
				5-HT _{1A}	5-HT _{2A}	5-HT ₃	5-HT ₄	5-HT ₇	D ₂	α_1
(±)-9		N		1.23 ± 0.09	>1000	>1000	>1000	299 ± 8	>1000	121 ± 2
24		N		8.2 ± 0.5	>1000	>1000	>1000	60 ± 9	>1000	54 ± 3
25		N		12.9 ± 0.7	>1000	>1000	>1000	94 ± 13	>1000	7.2 ± 0.8
26		N		5.9 ± 0.5	>1000	>1000	>1000	7.6 ± 0.6	>1000	14 ± 1
27		N		87.6 ± 0.4	nd	nd	nd	nd	nd	nd
28		N		27 ± 3	>1000	>1000	>1000	63 ± 6	>1000	69 ± 16
29		N		114 ± 13	nd	nd	nd	nd	nd	nd
30		N		>1000	nd	nd	nd	nd	nd	nd
31		N		28 ± 3	>1000	>1000	>1000	>1000	>1000	>1000
32		N		42 ± 3	>1000	>1000	>1000	>1000	40 ± 9	>1000
33	--	S		5.5 ± 0.4	>1000	>1000	>1000	123 ± 18	>1000	28 ± 4
34	--	S		1.3 ± 0.2	>1000	>1000	>1000	87 ± 3	>1000	26 ± 2
35	--	S		12.6 ± 0.5	>1000	12 ± 1	60 ± 7	12 ± 1	410 ± 71	25 ± 3

^aValues are the mean of two to four experiments performed in triplicate; nd, not determined.

further positions the amide subunit toward the extracellular solvent via the opening located between TMs 2 and 7. (ii) The *trans* configuration of spacer 1 is preferred over the *cis* configuration. (iii) The presence of Phe^{3,28} in the pathway toward the minor binding pocket permits the substitution of methylene units by a phenyl ring. (iv) The amide moiety, located in the minor binding pocket, forms hydrogen bond interactions with Tyr^{2,64}, Gln^{2,65}, and Trp^{7,40}. The flexibility of these large side chains and the putative presence of discrete water molecules, which play a crucial contribution to the ligand–receptor binding affinity,⁵² explain that modifications of the amide subunit do not have a significant influence in the binding affinity. (v) The aromatic ring of the chromane system (in gray) is positioned between Val^{3,33}, Trp^{6,48}, and Phe^{6,52}, occupying the orthosteric binding pocket (Figure 1B). Compounds 10–17 without this aromatic ring (single-ring Ar systems) cannot achieve these interactions, leading to inactive compounds (Table 1). The importance of these interactions is also revealed in the structure–affinity relationships of compounds 4–7. Figure 1C shows a detailed view of the bicyclic Ar systems of ligands 26 (white/gray), 4 (orange), 5 (olive), 6 (purple), and 7 (blue) in the orthosteric binding cavity of the 5-HT_{1A}R for comparison purposes. Clearly, all active compounds (5, 6, 7) position the aromatic ring in a similar manner to compound 26, facilitating the interaction with Trp^{6,48} and Phe^{6,52}. In contrast, the 1-naphthyl system of compound 4 is placed toward the extracellular side that impedes the key interactions with Trp^{6,48} and Phe^{6,52}, leading to an inactive analogue.

Functional Characterization at the 5-HT_{1A}R. The new identified high-affinity 5-HT_{1A}R ligands ($K_i < 25$ nM, Tables 2–4) were considered for further biological studies. Their functional role was characterized both *in vitro* and *in vivo*. The *in vitro* agonist action was studied by measuring the inhibition of forskolin-stimulated cyclic adenosine monophosphate

(cAMP) formation in HeLa cells transfected with the human 5-HT_{1A}R (h5-HT_{1A}R). The *in vivo* test of 5-HT_{1A}R stimulation consisted of the hypothermic response in mice (sensitive to the selective 5-HT_{1A}R antagonist WAY-100635). (±)-2, a 5-HT_{1A}R agonist with marked neuroprotection in animal models of ischemic stroke, was used as reference compound. Most of the assayed compounds behaved as pure agonists in the cell line transfected with the h5-HT_{1A}R, with EC₅₀ values for adenylyl cyclase inhibition in the range of 11.6–34.2 nM (Table 5). In general, a correlation between *in vitro* and *in vivo* potency was observed.

Neuroprotective Effect. *In Vitro* Assays. The *in vitro* neuroprotective effect was evaluated in primary neuronal cultures from rat hippocampus. Neurotoxicity assays consisted of determining the protection against cell death induced by serum deprivation, glutamate toxicity, or oxygen-glucose deprivation. The 5-HT_{1A}R agonist 1 and the neuroprotective agent 2 were also included in these studies for comparative purposes. The results show that some of the new 5-HT_{1A}R agonists afforded neuroprotection, similar to that of reference compounds, against cell death in primary hippocampal cultures exposed to serum and oxygen-glucose deprivation (Table 6). In particular, ligand (±)-9, endowed with high affinity ($K_i = 1.23$ nM, Table 1), selectivity (Table 2), and agonist potency (EC₅₀ = 16.3 nM, Table 5) for the 5-HT_{1A}R, was approximately equipotent to agonist 1 against apoptotic cell death induced by serum deprivation and against excitotoxic cell death (Table 6). However, all other new 5-HT_{1A}R agonists tested were virtually devoid of neuroprotective effect on neuronal cell death induced by glutamate. Notably, compounds 25 and 26 afforded a high neuroprotection against cell death in cultures exposed to oxygen–glucose deprivation, similar to that of reference compound (–)-2 (Table 6). It should be noted that, in general, the protective effect was not strictly concentration-dependent, so only the highest effect found is shown in the

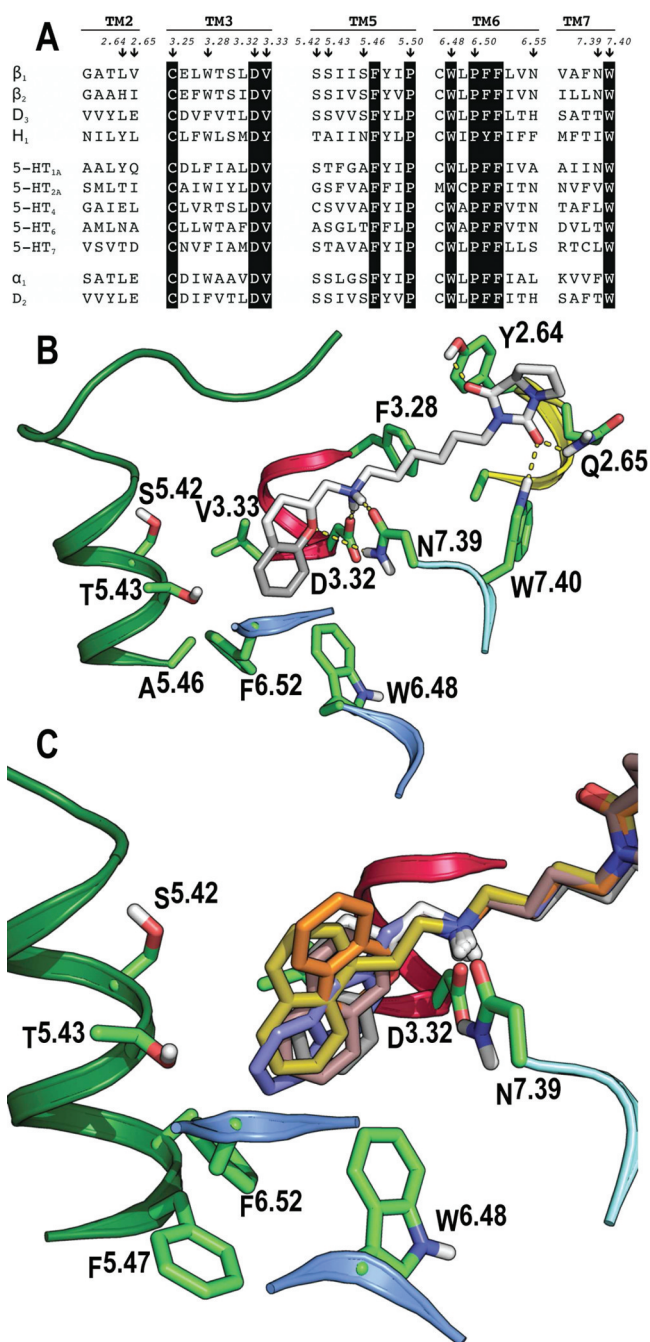


Figure 1. (A) Sequence alignment of TMs 2, 3, 5–7 of known crystal structures (β_1 - and β_2 -adrenergic receptors and dopamine D₃ and histamine H₁ receptors), serotonin 5-HT_{1A}, 5-HT_{2A}, 5-HT₄, 5-HT₆, and 5-HT₇ receptors, and α_1 and D₂ receptors. (B) Computational model of the complex between ligand **26** (in white, the aromatic ring of the chromane system is shown in gray) and a β_2 -based homology model of the 5-HT_{1A}R. In this model, the protonated amine and the oxygen atom of chromane anchors between Asp^{3.32} and Asn^{7.39}, the aromatic ring of chromane interacts with Val^{3.33} and Trp^{6.48}, and 1,3-dioxoperhydropyrrolo[1,2-*c*]imidazole forms hydrogen bond interactions with Tyr^{2.64}, Gln^{2.65}, and Trp^{7.40}. (C) Detailed view of the bicyclic aromatic systems of ligands **26** (white/gray), **4** (orange), **5** (olive), **6** (purple), and **7** (blue) in the orthosteric binding cavity of the 5-HT_{1A}R.

table. Such a lack of a concentration- or dose-dependent effect has been reported for other 5-HT_{1A}R agonists in previous studies.^{53,54}

Table 5. Functional Characterization of New 5-HT_{1A}R Agonists

compd	inhibition of cAMP formation (HeLa cells)		hypothermia (minimal effective dose, mg/kg)
	EC ₅₀ (nM)	maximum effect (%)	
8	(PA)	75.8	nd
(±)-9	16.3	94.6	2.5
18	(PA) ^a	77.9	nd
19	123	87.6	nd
21	18.9	94.5	1.3
22	31.5	89.3	2.5
23	11.6	89.6	0.30
24	23.3	94.3	0.62
25	157	92.5	5.0
26	21.8	91.2	2.5
33	34.2	94.8	1.3
34	19.9	87.0	1.3
35	25.9	88.6	5.0
(±)-2	1.5	94.8	0.15

^aBiphasic effect; (PA), partial agonist; nd, not determined.

Table 6. In Vitro Neuroprotective Effect of New 5-HT_{1A}R Agonists in Primary Neuronal Cultures from Rat Hippocampus

compd	concentration (μ M) ^a	protection (%) ^b		
		serum deprivation	glutamate toxicity	oxygen-glucose deprivation
(±)-9	1	41 ± 7	37 ± 5	21 ± 2
19	10	13 ± 4	nd	66 ± 5
21	10	0	0	nd
22	10	0	0	nd
23	0.1	23 ± 3	7 ± 2	
24	1	36 ± 3	nd	35 ± 7
25	0.1	16 ± 2	0	78 ± 7
26	0.1	30 ± 3	0	78 ± 7
33	10	21 ± 3	0	10 ± 3
34	10	28 ± 2	0	9 ± 5
35	1	32 ± 4	nd	32 ± 8
1	1	44 ± 1	37 ± 3	54 ± 4
(-)-2	0.1	31 ± 3	nd	78 ± 9
(±)-2	0.1	26 ± 3	16 ± 1	nd

^aNeuroprotection was not generally concentration-related so only the lower concentration that induces the highest neuroprotective effect is shown. ^bCompounds were tested at concentrations from 1 nM to 10 μ M; nd, not determined.

In Vivo Models. Compound **26**, behaving as an effective neuroprotective agent in vitro, was subsequently tested in an in vivo model of neuroprotection. The selected animal model was the focal ischemia in rats induced by the permanent occlusion of the middle cerebral artery (MCAO), which represents an adequate model for ischemic stroke in humans. One day later, brain sections were stained with the mitochondrial dye 2,3,5-triphenyltetrazolium chloride (TTC), and cortical and subcortical infarct volumes were calculated by image analysis. Tested compounds were administered by continuous iv infusion. In these in vivo experiments, the 5-HT_{1A}R agonist **(-)-2**, previously reported as neuroprotective agent, was also assayed for comparative purposes. The results are shown in Table 7.

Table 7. Effect of New 5-HT_{1A}R Agonists (iv infusion) on Cerebral Infarct Induced by MCAO in the Rat

compd	dose ($\mu\text{g}/\text{kg}/\text{h}$)	(n)	infarct volume (mm^3)		
			total	cortical	subcortical
saline		(10)	546 \pm 51	399 \pm 38	147 \pm 23
26	40	(10)	387 \pm 47 ^a	263 \pm 41 ^a	124 \pm 14
(-)-2	40	(8)	377 \pm 58 ^a	271 \pm 55	106 \pm 9

^a*p* < 0.05 vs control (Student's *t*-test).

Administration of a low dose (40 $\mu\text{g}/\text{kg}/\text{h}$) of compound **26** for 4 h immediately after MCAO significantly reduced the total infarct volume measured 24 h later (~29% reduction), compared to the corresponding saline-treated controls. The protective effect was more marked in cortical areas (~35% protection) than in subcortical nuclei, where the protection did not reach statistical significance. Virtually identical results were obtained with the same dose (40 $\mu\text{g}/\text{kg}/\text{h}$) of reference agent (-)-2 infused over 4 h (Table 7). The results herein reported suggest the interest of further pharmacological development of compound **26** and related drugs.

CONCLUSIONS

Herein we report the synthesis of new compounds **4–35**, based on systematic modifications of different structural moieties present in the previously reported lead arylpiperazine **3**: the amide subunit, spacer 1, spacer 2, and the aromatic system (Chart 2). The new nonpiperazine derivatives were assessed for binding affinity at the 5-HT_{1A}R and selectivity over other serotonin receptors (Tables 1–4). Computational β_2 -based homology models revealed that ligands occupy the orthosteric pocket of the receptor between TMs 3, 5–7, and a minor binding pocket between TMs 2 and 7, explaining the observed structure–affinity relationships. Determination of the functional activity at the h5-HT_{1A}R receptor revealed that identified high-affinity ligands ($K_i < 25$ nM) represent second-generation 5-HT_{1A}R agonists (Table 5). New characterized 5-HT_{1A}R agonists were also evaluated for their potential in vitro and in vivo neuroprotective properties. Compounds (\pm)-**9**, **25**, and **26** afforded protection against cell death in neurotoxicity assays in primary neuronal cultures from rat hippocampus (Table 6). Interestingly, in the rat model of focal ischemia, iv infusion of compound **26** after MCAO significantly reduced the cerebral infarct volume (~29%), the protection being more marked in cortical areas (~35%). The protective effect of **26** was virtually identical to that of compound (-)-**2**, a 5-HT_{1A}R agonist that has been previously described as a neuroprotective agent (Table 7). Thus, new compound **26** [$X = (\text{CH}_2)_3$, $Y = \text{N}$, $n = 0$, $Z = (\text{CH}_2)_6$, $m = 1$, Ar = chroman-2-yl] has been characterized as a high-affinity and potent 5-HT_{1A}R agonist ($K_i = 5.9$ nM, $\text{EC}_{50} = 21.8$ nM) that exhibits in vitro and in vivo neuroprotective properties. The results herein reported suggest the interest of further pharmacological development of compound **26** and related drugs.

EXPERIMENTAL SECTION

Chemistry. Melting points (mp, uncorrected) were determined on a Stuart Scientific electrothermal apparatus. Infrared (IR) spectra were measured on a Shimadzu-8300 or Bruker Tensor 27 instrument equipped with a Specac ATR accessory of 5200–650 cm^{-1} transmission range; frequencies (ν) are expressed in cm^{-1} . Nuclear magnetic resonance (NMR) spectra were recorded on a Bruker

Avance 500 (¹H, 500 MHz; ¹³C, 125 MHz), Bruker Avance 300-AM (¹H, 300 MHz; ¹³C, 75 MHz) or Bruker 200-AC spectrometer (¹H, 200 MHz; ¹³C, 50 MHz) at the UCM's NMR facilities. Chemical shifts (δ) are expressed in parts per million relative to internal tetramethylsilane; coupling constants (*J*) are in hertz (Hz). The following abbreviations are used to describe peak patterns when appropriate: s (singlet), d (doublet), t (triplet), qt (quintet), m (multiplet), br (broad). 2D NMR experiments (HMQC and HMBC) of representative compounds were carried out to assign protons and carbons of the new structures. Elemental analyses (C, H, N or C, H, N, S) were obtained on a LECO CHNS-932 apparatus at the UCM's analysis services and were within 0.5% of the theoretical values, confirming a purity of at least 95% for all tested compounds. Optical rotations were recorded on a Perkin-Elmer 241 polarimeter using a 1 dm path length; concentrations are given as g/100 mL. Analytical thin-layer chromatography (TLC) was run on Merck silica gel plates (Kieselgel 60 F-254) with detection by UV light (254 nm), ninhydrin solution, or 10% phosphomolybdic acid solution in ethanol. Flash chromatography was performed on glass column using silica gel type 60 (Merck, particle size 230–400 mesh, for final compounds) or on a Varian 971-FP flash purification system using silica gel cartridges (Varian, particle size 50 μm , for intermediates). Unless stated otherwise, starting materials, reagents, and solvents were purchased as high-grade commercial products from Sigma-Aldrich, Acros, Lancaster, Scharlab, or Panreac and were used without further purification. Anhydrous tetrahydrofuran (THF) was distilled from sodium benzophenone ketyl and used immediately.

The following compounds were synthesized according to described procedures: tetrahydro-1*H*-pyrrolo[1,2-*c*]imidazole-1,3(2*H*)-dione (**36**),⁵⁵ tetrahydroimidazo[1,5-*a*]pyridine-1,3(2*H*,5*H*)-dione (**37**),³⁵ 1*H*-imidazo[1,5-*c*][1,3]thiazole-5,7(6*H*,7*aH*)-dione (**38**),³⁶ hexahydropyrrolo[1,2-*a*]pyrazine-1,4-dione (**40**),⁵⁶ tetrahydro-2*H*-pyrido[1,2-*a*]pyrazine-1,4(3*H*,6*H*)-dione (**41**),⁵⁶ 2-(4-bromobutyl)-tetrahydro-1*H*-pyrrolo[1,2-*c*]imidazole-1,3(2*H*)-dione (**42**),²⁵ 2-(4-bromobutyl)tetrahydroimidazo[1,5-*a*]pyridine-1,3(2*H*,5*H*)-dione (**43**),²⁵ 2-(4-bromobutyl)hexahydropyrrolo[1,2-*a*]pyrazine-1,4-dione (**44**),²⁷ 2-(4-bromobutyl)tetrahydro-2*H*-pyrido[1,2-*a*]pyrazine-1,4(3*H*,6*H*)-dione (**45**),²⁷ 2-(3-bromopropyl)tetrahydro-1*H*-pyrrolo[1,2-*c*]imidazole-1,3(2*H*)-dione (**49**),²⁵ 2-(1-naphthyl)ethylamine (**61**),³⁸ 2-(2-naphthyl)ethylamine (**62**),³⁸ quinolin-2-ylmethylamine (**63**),³⁹ 3,4-dihydro-2*H*-chromen-2-ylmethylamine (**64**),⁵⁷ and ethyl chromane-2-carboxylate ((\pm)-**65**).⁴¹ Collected data for compounds **4–35** refer to free bases, and then hydrochloride salts were prepared prior to mp determination, elemental analyses, and biological assays. Spectroscopic data of all described compounds were consistent with the proposed structures. For final compounds **4–35**, we include the data of **4**, **8**, **9**, **12**, **16**, **19**, **21**, **23**, **28**, **31**, and **34**. For intermediates **46–48** and **50–60**, the data of compounds **46**, **53**, **55**, and **56** are described.

Synthesis of Dihydroimidazo[5,1-*b*][1,3]thiazole-5,7(6*H*,7*aH*)-dione (39**).** To a suspension of 1,3-thiazolidine-2-carboxylic acid (3.45 g, 26 mmol) in H₂O (10 mL), potassium cyanate (3.00 g, 37 mmol) was added and the mixture was refluxed for 4 h, acidified with concentrated HCl to pH 2, and refluxed for an additional 2 h. The solvent was evaporated under reduced pressure, and the residue was dried under vacuum overnight. The crude was purified by continuous extraction with EtOAc to afford hydantoin **39** in 60% yield; mp 112–114 °C (EtOAc). IR (KBr) ν 3219, 1772, 1718. ¹H NMR (DMSO-*d*₆) δ 2.86–3.18 (m, 3H, 3/2CH₂), 4.20–4.30 (m, 1H, 1/2CH₂), 5.30 (s, 1H, CH), 11.40 (br s, 1H, NH). ¹³C NMR (DMSO-*d*₆) δ 32.4, 47.8 (2CH₂), 63.9 (CH), 159.8, 173.1 (2CO).

General Procedure for the Synthesis of Haloalkyl Derivatives **42–60.** To a suspension of 1 equiv of 1,3-thiazolidine-2,4-dione, hydantoin **36–39** or diketopiperazines **40,41** in anhydrous DMF (1.2 mL/mmol), 1 equiv of NaH (60% in mineral oil) was added at room temperature and under an argon atmosphere. The reaction mixture was stirred at 60 °C for 1 h, and a solution of 2 equiv of the corresponding α,ω -dibromo or -dichloro derivative in anhydrous DMF (0.5 mL/mmol) was added dropwise. The reaction was heated at 110 °C for 3 h. Then, the solvent was removed under

reduced pressure and the residue was suspended in H₂O and extracted with dichloromethane (3 × 50 mL). The combined organic layers were dried (Na₂SO₄), and the solvent was evaporated to dryness. The residue was purified by column chromatography using the appropriate eluent, to afford pure 42–60.

2-(4-Bromobutyl)tetrahydro-1H-pyrrolo[1,2-c]imidazole-1,3(2H)-dione (42). Obtained from 36 and 1,4-dibromobutane in 55% yield. Chromatography: hexane/EtOAc, 1:1.²⁵

2-(4-Bromobutyl)tetrahydroimidazol[1,5-a]pyridine-1,3(2H,5H)-dione (43). Obtained from 37 and 1,4-dibromobutane in 74% yield. Chromatography: hexane/EtOAc, 1:1.²⁵

2-(4-Bromobutyl)hexahydro-1H-cyclopenta[c]pyridine-1,4(4aH)-dione (44). Obtained from 40 and 1,4-dibromobutane in 55% yield. Chromatography: hexane/EtOAc, 2:8.²⁷

2-(4-Bromobutyl)octahydroisoquinoline-1,4-dione (45). Obtained from 41 and 1,4-dibromobutane in 45% yield. Chromatography: hexane/EtOAc, 2:8.²⁷

6-(4-Bromobutyl)-dihydroimidazo[5,1-b][1,3]thiazole-5,7-(6H,7aH)-dione (46). Obtained from 39 and 1,4-dibromobutane in 60% yield. Chromatography: hexane/EtOAc, 8:2. *R*_f (hexane/EtOAc, 8:2) 0.32. IR (CHCl₃) ν 1780, 1712. ¹H NMR (CDCl₃) δ 1.72–1.89 (m, 4H, (CH₂)₂), 2.92–3.18 (m, 3H, 3/2CH₂_{cyc}), 3.40 (t, *J* = 6.4, 2H, CH₂Br), 3.52 (t, *J* = 6.8, 2H, CH₂N), 4.48 (ddd, *J* = 12.3, 6.4, 2.0, 1H, 1/2CH₂_{cyc}), 5.07 (s, 1H, CH_{cyc}). ¹³C NMR (CDCl₃) δ 26.5, 29.6, 32.6, 32.8, 38.4, 49.3 (6CH₂), 64.5 (CH), 159.5, 171.8 (2CO).

6-(4-Bromobutyl)-1H-imidazo[1,5-c][1,3]thiazole-5,7(6H,7aH)-dione (47). Obtained from 38 and 1,4-dibromobutane in 65% yield. Chromatography: hexane/EtOAc, 8:2.

3-(4-Bromobutyl)-1,3-thiazolidine-2,4-dione (48). Obtained from 1,3-thiazolidine-2,4-dione and 1,4-dibromobutane in 62% yield. Chromatography: hexane/EtOAc, 8:2.

2-(3-Bromopropyl)tetrahydro-1H-pyrrolo[1,2-c]imidazole-1,3(2H)-dione (49). Obtained from 36 and 1,3-dibromopropane in 67% yield. Chromatography: hexane/EtOAc, 8:2.²⁵

2-(5-Bromopentyl)tetrahydro-1H-pyrrolo[1,2-c]imidazole-1,3(2H)-dione (50). Obtained from 36 and 1,5-dibromopentane in 50% yield. Chromatography: hexane/EtOAc, 1:1.

2-(6-Bromohexyl)tetrahydro-1H-pyrrolo[1,2-c]imidazole-1,3(2H)-dione (51). Obtained from 36 and 1,6-dibromohexane in 55% yield. Chromatography: hexane/EtOAc, 1:1.

2-(8-Bromooctyl)tetrahydro-1H-pyrrolo[1,2-c]imidazole-1,3(2H)-dione (52). Obtained from 36 and 1,8-dibromooctane in 62% yield. Chromatography: hexane/EtOAc, 8:2.

2-[(2E)-4-Bromobut-2-enyl]tetrahydro-1H-pyrrolo[1,2-c]imidazole-1,3(2H)-dione (53). Obtained from 36 and (2E)-1,4-dibromobut-2-ene in 43% yield. Chromatography: hexane/EtOAc, 8:2. *R*_f (hexane/EtOAc, 8:2) 0.20. IR (CHCl₃) ν 1772, 1713. ¹H NMR (CDCl₃) δ 1.61–1.79 (m, 1H, 1/2CH₂_{cyc}), 1.97–2.34 (m, 3H, 3/2CH₂_{cyc}), 3.25 (ddd, *J* = 11.2, 7.6, 5.4, 1H, 1/2CH₂_{cyc}), 3.69 (dt, *J* = 11.2, 7.6, 1H, 1/2CH₂_{cyc}), 3.91 (d, *J* = 6.8, 2H, CH₂Br/CH₂N), 4.07–4.17 (m, 3H, CH₂Br/CH₂N, CH_{cyc}), 5.59–5.99 (m, 2H, CH=CH). ¹³C NMR (CDCl₃) δ 26.8, 27.4, 31.0, 39.4, 45.3 (5CH₂), 63.3, 127.7, 130.1 (3CH), 160.9, 173.3 (2CO).

2-[(2Z)-4-Chlorobut-2-enyl]tetrahydro-1H-pyrrolo[1,2-c]imidazole-1,3(2H)-dione (54). Obtained from 36 and (2Z)-1,4-dichlorobut-2-ene in 55% yield. Chromatography: hexane/EtOAc, 8:2.

2-(4-Chlorobut-2-ynyl)tetrahydro-1H-pyrrolo[1,2-c]imidazole-1,3(2H)-dione (55). Obtained from 36 and 1,4-dichlorobut-2-yne in 58% yield. Chromatography: hexane/EtOAc, 8:2. *R*_f (hexane/EtOAc, 8:2) 0.14. IR (CHCl₃) ν 1776, 1719. ¹H NMR (CDCl₃) δ 1.61–1.81 (m, 1H, 1/2CH₂_{cyc}), 1.98–2.35 (m, 3H, 3/2CH₂_{cyc}), 3.27 (ddd, *J* = 11.2, 7.6, 5.1, 1H, 1/2CH₂_{cyc}), 3.71 (dt, *J* = 11.2, 7.6, 1H, 1/2CH₂_{cyc}), 4.09–4.17 (m, 3H, CH₂N/CH₂Br, CH_{cyc}), 4.29 (s, 2H, CH₂N/CH₂Br). ¹³C NMR (CDCl₃) δ 27.0, 27.4, 28.3, 30.1, 45.5 (5CH₂), 63.5 (CH), 99.3, 99.7 (2C), 159.1, 172.6 (2CO).

2-(4-(Bromomethyl)benzyl)tetrahydro-1H-pyrrolo[1,2-c]imidazole-1,3(2H)-dione (56). Obtained from 36 and 1,4-bis-(bromomethyl)benzene in 40% yield. Chromatography: hexane/EtOAc, 7:3. *R*_f (hexane/EtOAc, 8:2) 0.20. IR (CHCl₃) ν 1773, 1713. ¹H NMR (CDCl₃) δ 1.59–1.75 (m, 1H, 1/2CH₂_{cyc}), 1.94–2.31 (m, 3H, 3/2CH₂_{cyc}), 3.22 (ddd, *J* = 11.2, 7.6, 5.4, 1H, 1/2CH₂_{cyc}), 3.66

(dt, *J* = 11.2, 7.6, 1H, 1/2CH₂_{cyc}), 4.07 (dd, *J* = 9.0, 7.6, 1H, CH_{cyc}), 4.45 (s, 2H, CH₂Br/CH₂N), 4.59 (s, 2H, CH₂Br/CH₂N), 7.33 (m, 4H, 4CH_{Ar}). ¹³C NMR (CDCl₃) δ 27.1, 27.6, 33.2, 42.2, 45.6 (5CH₂), 63.6 (CH), 129.1, 129.3, 129.5, 129.6 (4CH), 136.4, 137.5 (2C), 160.4, 173.6 (2CO).

2-[3-(Bromomethyl)benzyl]tetrahydro-1H-pyrrolo[1,2-c]imidazole-1,3(2H)-dione (57). Obtained from 36 and 1,3-bis-(bromomethyl)benzene in 42% yield. Chromatography: hexane/EtOAc, 8:2.

3-(5-Bromopentyl)-1,3-thiazolidine-2,4-dione (58). Obtained from 1,3-thiazolidine-2,4-dione and 1,5-dibromopentane in 61% yield. Chromatography: hexane/EtOAc, 9:1.

3-(6-Bromohexyl)-1,3-thiazolidine-2,4-dione (59). Obtained from 1,3-thiazolidine-2,4-dione and 1,6-dibromohexane in 45% yield. Chromatography: hexane/EtOAc, 8:2.

3-(8-Bromooctyl)-1,3-thiazolidine-2,4-dione (60). Obtained from 1,3-thiazolidine-2,4-dione and 1,8-dibromooctane in 50% yield. Chromatography: hexane/EtOAc, 9:1.

Synthesis of Ethyl (2R)-(-) and (2S)-(+)-Chromane-2-carboxylate ((-)- and (+)-65). To a solution of racemic ethyl chromane-2-carboxylate ((±)-65) (5.00 g, 24.2 mmol) in THF (20 mL), ion-free H₂O (140 mL) and 0.05 M phosphate buffer (133 mL, pH 7.0) were added, and the mixture was raised to pH 8.0 with an aqueous solution of 0.1 M NaOH, at room temperature. Then, lipase P-30 (194 mg, 309 U/mg) was added in portions while the reaction was vigorously stirred and the pH was kept at 8.0 by addition of an aqueous solution of 0.01 M NaOH (about 1.5 L). When pH was stable at 8.0, THF was evaporated and the aqueous mixture was extracted with EtOAc (3 × 750 mL). The organic layers were dried (Na₂SO₄) and evaporated to afford enantiopure ester (-)-65 as an oil in 42% yield: [α]_D²⁰ -8.7 (c 1.24, MeOH) (lit.⁵⁸ [α]_D²⁰ -9.3 (c 1.24, MeOH)). IR, ¹H, and ¹³C NMR spectra were consistent with those described for racemic (±)-65. The enantiomeric excess (ee) was determined by chiral HPLC analysis carried out on an Agilent 1200 series system (Chiralpak IC, hexane/*i*-PrOH 95:5, 1.2 mL/min, 38 bar, 280 nm); (S)-enantiomer *t*_r = 7.93 min (minor); (R)-enantiomer *t*_r = 11.71 min (major): 97% ee. The aqueous layer was acidified with concentrated HCl to pH 1.0 and extracted with EtOAc (3 × 750 mL). The organic layers were dried (Na₂SO₄) and evaporated to afford the free carboxylic acid, which was esterified by treatment with EtOH and H₂SO₄ at reflux for 2 h. The solvent was evaporated, and the residue was suspended in dichloromethane and washed with a saturated aqueous solution of NaHCO₃ and brine. The organic layer was dried (Na₂SO₄) and evaporated to afford ester 65, which was resubjected to enzymatic hydrolysis with lipase P30 for optical purity enhancement. Following the hydrolysis procedure previously described, (2S)-(+)-chromanecarboxylic acid was obtained. Then, this acid was esterified as described previously in this experiment to afford enantiopure ester (+)-65 as an oil in 38% global yield: [α]_D²⁰ +8.6 (c 1.24, MeOH) (lit.⁵⁸ [α]_D²⁰ +9.3 (c 1.24, MeOH)) (95% ee).

Synthesis of (2R)-(-) and (2S)-(+)-3,4-dihydro-2H-chromen-2-ylmethylamine ((-)- and (+)-64). To a mixture of enantiopure ester (-)- or (+)-65 (4.7 g, 22.6 mmol) and ammonium chloride (280 mg, 5.5 mmol), aqueous 28% ammonia (63 mL) was added and the mixture was heated at 100 °C for 2 h. After cooling to room temperature, H₂O was added (50 mL) and the solution was extracted with dichloromethane (3 × 75 mL). The combined organic layers were dried (Na₂SO₄) and evaporated to afford (2R)-(-)- or (2S)-(-)-chromane-2-carboxamide as a white solid in 70% and 72% yield, respectively, which were used in the next step without further purification. (2R)-(-)-Chromane-2-carboxamide: [α]_D²⁰ +39.8 (c 1.2, MeOH). *R*_f (hexane/EtOAc, 1:9) 0.31. IR (KBr) ν 3400, 1662, 1608, 1581, 1488, 1456. ¹H NMR (DMSO-*d*₆) δ 1.82–1.98 (m, 1H, 1/2CH₂CH), 2.09–2.23 (m, 1H, 1/2CH₂CH), 2.62–2.89 (m, 2H, CH₂Ar), 4.47 (dd, *J* = 8.8, 3.2, 1H, CH), 6.79–6.87 (m, 2H, 2CH_{Ar}), 7.04–7.13 (m, 2H, 2CH_{Ar}), 7.38 (br s, 1H, CONH), 7.43 (br s, 1H, CONH). ¹³C NMR (DMSO-*d*₆) δ 23.2, 24.2 (2CH₂), 74.5, 116.5, 120.3 (3CH), 121.9 (C), 127.0, 129.4 (2CH), 153.2 (C), 172.2 (CO). (2S)-(-)-Chromane-2-carboxamide: [α]_D²⁰ -37.5 (c 1.2, MeOH).

To an ice-cooled solution of 1 M diborane in THF (45 mL, 45 mmol), a solution of (2*R*)-(+)- or (2*S*)-(-)-chromane-2-carboxamide (2.11 g, 11.9 mmol) in anhydrous THF (55 mL) was added dropwise under an argon atmosphere, and the mixture was stirred at room temperature overnight. Then, the reaction mixture was refluxed for 1 h and, after cooling to room temperature, 10% HCl (3.4 mL) was added. The solvent was evaporated, and the residue was basified to pH 8.5 with aqueous 10% NaOH and extracted with Et₂O (6 × 50 mL). The combined organic layers were dried (Na₂SO₄) and evaporated. The residue was purified by column chromatography (dichloromethane/EtOH, 9:1) to afford the corresponding amines (-)-**64** or (+)-**64** in 82 and 86% yield, respectively. (-)-**64**: oil. [α]_D²⁰ -119.5 (c 1.0, THF) (lit.⁵⁹ [α]_D²⁰ -122.8 (c 1.0, THF)). R_f (dichloromethane/EtOH, 9:1): 0.35. IR (CHCl₃) ν 3387, 1608, 1581, 1489, 1456. ¹H NMR (CDCl₃) δ 1.69–1.97 (m, 2H, CH₂CH), 2.70–2.88 (m, 2H, CH₂Ar), 2.92 (d, J = 7.3, 2H, CH₂NH₂), 3.95 (dtd, J = 10.3, 5.5, 2.4, 1H, CH), 6.81 (m, 2H, 2CH_{Ar}), 7.04–7.13 (m, 2H, 2CH_{Ar}). ¹³C NMR (CDCl₃) δ 24.6, 25.0, 46.6 (3CH₂), 77.4, 116.6, 120.1 (3CH), 121.9 (C), 127.2, 129.5 (2CH), 154.7 (C). (+)-**64**: oil. [α]_D²⁰ +110.5 (c 1.0, THF) (lit.⁵⁹ [α]_D²⁰ +128.8 (c 1.0, THF)).

General Procedure for the Synthesis of Final Compounds 4–35. To a solution of 4 equiv of the corresponding arylalkylamine (commercially available or **61–64**) in dry acetonitrile (1 mL/mmol), a solution of 1 equiv of the appropriate bromo- or chloroalkyl derivative **42–60** in dry acetonitrile (4 mL/mmol) was added dropwise and under an argon atmosphere. The reaction mixture was stirred at 60 °C overnight. Once at room temperature, the solvent was removed under reduced pressure and the residue was suspended in an aqueous solution of 20% K₂CO₃ and extracted with dichloromethane (3 × 50 mL). The organic layer was dried (Na₂SO₄), and the solvent was evaporated to dryness. The residue was purified by column chromatography using the appropriate eluent, to afford pure **4–35**. The free amine was characterized (yield, R_f, IR, NMR), dissolved in anhydrous Et₂O (6 mL/mmol), and a commercial 1 M HCl(g)/Et₂O solution (3 mL/mmol) was added. The hydrochloride salt was isolated by filtration or evaporation, washed with anhydrous Et₂O, dried under high vacuum, and characterized (mp, elemental analysis).

2-[4-[(1-Naphthylmethyl)amino]butyl]tetrahydro-1*H*-pyrrolo[1,2-*c*]imidazole-1,3(2*H*)-dione (4**).** Obtained from **42** and 1-naphthylmethylamine in 42% yield. Chromatography: EtOAc; mp 150–153 °C (chloroform/hexane). IR (CHCl₃) ν 3500, 3300, 1770, 1708. ¹H NMR (CDCl₃) δ 1.48–1.71 (m, 5H, (CH₂)₂, 1/2CH₂cy_c), 1.99–2.08 (m, 2H, CH₂cy_c), 2.16–2.24 (m, 1H, 1/2CH₂cy_c), 2.74 (t, J = 6.9, 2H, CH₂NH), 3.16–3.24 (m, 1H, 1/2CH₂cy_c), 3.47 (t, J = 6.9, 2H, CH₂N), 3.64 (dt, J = 11.1, 7.8, 1H, 1/2CH₂cy_c), 4.02 (dd, J = 9.3, 7.8, 1H, CH₂cy_c), 4.20 (s, 2H, CH₂Ar), 7.37–7.54 (m, 4H, 4CH_{Ar}), 7.74 (d, J = 7.2, 1H, CH_{Ar}), 7.82–7.85 (m, 1H, CH_{Ar}), 8.08 (d, J = 8.4, 1H, CH_{Ar}). ¹³C NMR (CDCl₃) δ 25.9, 27.0, 27.2, 27.5, 38.8, 45.5, 49.3, 51.6 (8CH₂), 63.3, 123.6, 125.4, 125.6, 126.1, 127.7, 128.7 (8CH), 131.8, 133.9, 136.0 (3C), 160.9, 173.9 (2CO). Anal. (C₂₁H₂₃N₃O₂·HCl) C, H, N.

2-[4-[(2-(1-Naphthyl)ethyl)amino]butyl]tetrahydro-1*H*-pyrrolo[1,2-*c*]imidazole-1,3(2*H*)-dione (5**).** Obtained from **42** and amine **61** in 35% yield. Chromatography: EtOAc/EtOH, 1:1.

2-[4-[(2-Naphthylmethyl)amino]butyl]tetrahydro-1*H*-pyrrolo[1,2-*c*]imidazole-1,3(2*H*)-dione (6**).** Obtained from **42** and 2-naphthylmethylamine in 44% yield. Chromatography: dichloromethane/EtOH, 95:5.

2-[4-[(2-(2-Naphthyl)ethyl)amino]butyl]tetrahydro-1*H*-pyrrolo[1,2-*c*]imidazole-1,3(2*H*)-dione (7**).** Obtained from **42** and amine **62** in 35% yield. Chromatography: EtOAc/EtOH, 9:1.

2-[4-[(Quinolin-2-ylmethyl)amino]butyl]tetrahydro-1*H*-pyrrolo[1,2-*c*]imidazole-1,3(2*H*)-dione (8**).** Obtained from **42** and amine **63** in 40% yield. Chromatography: EtOAc/EtOH, 7:3; mp 126–127 °C (EtOAc). R_f (EtOAc/EtOH, 7:3) 0.21. IR (CHCl₃) ν 3362, 1770, 1708. ¹H NMR (CDCl₃) δ 1.52–1.67 (m, 5H, (CH₂)₂, 1/2CH₂cy_c), 1.90–2.27 (m, 3H, 3/2CH₂cy_c), 2.50 (t, J = 6.3, 2H, CH₂NH), 3.01–3.24 (m, 1H, 1/2CH₂cy_c), 3.42 (t, J = 6.8, 2H, CH₂N), 3.53–3.69 (m, 1H, 1/2CH₂cy_c), 3.91–4.00 (m, 3H, CH₂Ar, CH₂cy_c), 7.47 (t, J = 7.1, 1H, CH_{Ar}), 7.62–7.77 (m, 3H, 3CH_{Ar}), 8.02 (d, J = 8.3, 1H, CH_{Ar}),

8.11 (d, J = 8.5, 1H, CH_{Ar}). ¹³C NMR (CDCl₃) δ 24.4, 25.8, 26.8, 27.4, 38.7, 45.4, 53.8, 54.1 (8CH₂), 63.1, 120.9, 126.0, 127.2, 128.9 (5CH), 129.1 (C), 129.2 136.2 (2CH), 147.4 (C), 160.5, 160.7 (C, CO), 173.8 (CO). Anal. (C₂₀H₂₄N₄O₂·HCl) C, H, N.

(±)-2-[4-[(3,4-Dihydro-2*H*-chromen-2-ylmethyl)amino]butyl]tetrahydro-1*H*-pyrrolo[1,2-*c*]imidazole-1,3(2*H*)-dione ((±)-9**).** Obtained from **42** and racemic amine **64** in 37% yield. Chromatography: EtOAc/EtOH, 8:2; oil. R_f (dichloromethane/EtOH, 9:1) 0.28. IR (CHCl₃) ν 3405, 1772, 1709. ¹H NMR (CDCl₃) δ 1.47–1.86 (m, 5H, (CH₂)₂, 1/2CH₂cy_c), 1.91–2.12 (m, 4H, CH₂cy_c, CH₂chrom), 2.16–2.34 (m, 1H, 1/2CH₂cy_c), 2.64–2.92 (m, 6H, 2CH₂NH, CH₂chrom), 3.16–3.28 (m, 1H, 1/2CH₂cy_c), 3.48 (t, J = 7.1, 2H, CH₂N), 3.66 (dt, J = 11.2, 7.3, 1H, 1/2CH₂cy_c), 4.05 (dd, J = 9.1, 7.3, 1H, CH₂cy_c), 4.11–4.18 (m, 1H, CH_{chrom}), 6.81 (t, J = 7.6, 2H, 2CH_{Ar}), 7.00–7.10 (m, 2H, 2CH_{Ar}). ¹³C NMR (CDCl₃) δ 24.6, 25.6, 25.8, 26.9, 27.1, 27.5, 38.7, 45.4, 49.3, 54.1 (10CH₂), 63.2, 75.0, 116.7, 120.1 (4CH), 121.9 (C), 127.1, 129.4 (2CH), 154.5 (C), 160.8, 173.9 (2CO). Anal. (C₂₀H₂₇N₃O₃·HCl·H₂O) C, H, N.

(+)-2-[4-[(2*S*)-3,4-Dihydro-2*H*-chromen-2-ylmethyl]amino]butyl]tetrahydro-1*H*-pyrrolo[1,2-*c*]imidazole-1,3(2*H*)-dione ((+)-9**).** Obtained from **42** and enantiopure amine (+)-**64** in 38% yield; [α]_D²⁰ +65 (c 0.5, CHCl₃). IR, ¹H, and ¹³C NMR spectra were consistent with those reported for racemic **9**. Anal. (C₂₀H₂₇N₃O₃·HCl·3H₂O) C, H, N.

(-)-2-[4-[(2*R*)-3,4-Dihydro-2*H*-chromen-2-ylmethyl]amino]butyl]tetrahydro-1*H*-pyrrolo[1,2-*c*]imidazole-1,3(2*H*)-dione ((-)-9**).** Obtained from **42** and enantiopure amine (-)-**64** in 35% yield; [α]_D²⁰ -77 (c 0.5, CHCl₃). IR, ¹H, and ¹³C NMR spectra were consistent with those reported for racemic **9**. Anal. (C₂₀H₂₇N₃O₃·HCl) C, H, N.

2-[4-(Benzylamino)butyl]tetrahydro-1*H*-pyrrolo[1,2-*c*]imidazole-1,3(2*H*)-dione (10**).** Obtained from **42** and benzylamine in 45% yield. Chromatography: EtOAc.

2-[4-[(2-Phenylethyl)amino]butyl]tetrahydro-1*H*-pyrrolo[1,2-*c*]imidazole-1,3(2*H*)-dione (11**).** Obtained from **42** and 2-phenylethylamine in 48% yield. Chromatography: EtOAc.

2-[4-[(2-Furylmethyl)amino]butyl]tetrahydro-1*H*-pyrrolo[1,2-*c*]imidazole-1,3(2*H*)-dione (12**).** Obtained from **42** and 2-furylmethylamine in 38% yield. Chromatography: EtOAc; mp 135–136 °C (hexane/Et₂O). R_f (EtOAc/EtOH, 8:2) 0.32. IR (CHCl₃) ν 3462, 1771, 1709. ¹H NMR (CDCl₃) δ 1.38–1.71 (m, 5H, (CH₂)₂, 1/2CH₂cy_c), 1.98–2.22 (m, 3H, 3/2CH₂cy_c), 2.55 (t, J = 7.3, 2H, CH₂NH), 3.19 (ddd, J = 11.7, 7.4, 5.4, 1H, 1/2CH₂cy_c), 3.39 (t, J = 6.9, 2H, CH₂N), 3.58 (dt, J = 11.2, 7.4, 1H, 1/2CH₂cy_c), 3.70 (s, 2H, CH₂Ar), 3.99 (dd, J = 8.4, 7.4, 1H, CH₂cy_c), 6.07 (d, J = 3.1, 1H, CH_{Ar}), 6.24 (dd, J = 3.6, 1.9, 1H, CH_{Ar}), 7.28 (dd, J = 1.8, 0.8, 1H, CH_{Ar}). ¹³C NMR (CDCl₃) δ 25.6, 26.8, 26.9, 27.4, 38.6, 45.3, 45.9, 48.3, (8CH₂), 63.1, 106.6, 109.9, 141.6 (4CH), 153.7 (C), 160.6, 173.8 (2CO). Anal. (C₁₈H₂₁N₃O₃·HCl·H₂O) C, H, N.

2-[4-[(2-(2-Furyl)ethyl)amino]butyl]tetrahydro-1*H*-pyrrolo[1,2-*c*]imidazole-1,3(2*H*)-dione (13**).** Obtained from **42** and 2-(2-furyl)ethylamine in 36% yield. Chromatography: EtOAc.

2-[4-[(Thien-2-ylmethyl)amino]butyl]tetrahydro-1*H*-pyrrolo[1,2-*c*]imidazole-1,3(2*H*)-dione (14**).** Obtained from **42** and thien-2-ylmethylamine in 40% yield. Chromatography: EtOAc.

2-[4-[(2-Thien-2-ylethyl)amino]butyl]tetrahydro-1*H*-pyrrolo[1,2-*c*]imidazole-1,3(2*H*)-dione (15**).** Obtained from **42** and 2-(thien-2-yl)ethylamine in 35% yield. Chromatography: EtOAc.

2-[4-[(Pyridin-2-ylmethyl)amino]butyl]tetrahydro-1*H*-pyrrolo[1,2-*c*]imidazole-1,3(2*H*)-dione (16**).** Obtained from **42** and pyridin-2-ylmethylamine in 37% yield. Chromatography: EtOAc; oil. R_f (EtOAc) 0.05. IR (CHCl₃) ν 3385, 1771, 1709. ¹H NMR (CDCl₃) δ 1.49–1.84 (m, 5H, (CH₂)₂, 1/2CH₂cy_c), 1.95–2.32 (m, 3H, 3/2CH₂cy_c), 2.67 (t, J = 7.1, 2H, CH₂NH), 3.23 (ddd, J = 11.4, 7.3, 5.4, 1H, 1/2CH₂cy_c), 3.48 (t, J = 6.8, 2H, CH₂N), 3.67 (dt, J = 11.2, 7.6, 1H, 1/2CH₂cy_c), 3.89 (s, 2H, CH₂Ar), 4.06 (dd, J = 8.8, 7.6, 1H, CH₂cy_c), 7.16 (dd, J = 6.7, 5.0, 1H, CH_{Ar}), 7.26–7.31 (m, 1H, CH_{Ar}), 7.64 (td, J = 7.6, 1.5, 1H, CH_{Ar}), 8.54 (d, J = 4.6, 1H, CH_{Ar}). ¹³C NMR (CDCl₃) δ 25.9, 27.0, 27.2, 27.6, 38.8, 45.5, 49.0, 55.2 (8CH₂), 63.3, 121.9, 122.3, 136.4, 149.3 (SCH), 163.3 (C), 164.2, 175.9 (2CO). Anal. (C₁₆H₂₂N₄O₂·2HCl·SH₂O) C, H, N.

2-[4-[(2-Pyridin-2-ylethyl)amino]butyl]tetrahydro-1H-pyrrolo[1,2-c]imidazole-1,3(2H)-dione (17). Obtained from 42 and 2-(pyridin-2-yl)ethylamine in 36% yield. Chromatography: EtOAc.

2-[4-[(3,4-Dihydro-2H-chromen-2-ylmethyl)amino]butyl]tetrahydroimidazo[1,5-a]pyridine-1,3(2H,5H)-dione (18). Obtained from 43 and amine 64 in 35% yield. Chromatography: dichloromethane/EtOH, 9:1.

2-[4-[(3,4-Dihydro-2H-chromen-2-ylmethyl)amino]butyl]hexahydropyrrolo[1,2-a]pyrazine-1,4-dione (19). Obtained from 44 and amine 64 in 35% yield. Chromatography: EtOAc; oil. R_f (EtOAc/EtOH, 9:1) 0.40. IR (CHCl₃) ν 3422, 1663. ¹H NMR (CDCl₃) δ 1.14–2.09 (m, 9H, (CH₂)₂, 3/2CH₂_{cyo}, CH₂_{chrom}), 2.28–2.34 (m, 1H, 1/2CH₂_{cyo}), 2.65–2.93 (m, 6H, 2CH₂NH, CH₂_{chrom}), 3.29–3.56 (m, 4H, CH₂N, CH₂_{cyo}), 3.71 (d, J = 16.0, 1H, 1/2CH₂_{cyo}), 4.04–4.14 (m, 3H, CH_{chrom}, CH_{cyo}, 1/2CH₂_{cyo}), 6.67–6.80 (m, 2H, 2CH_{Ar}), 6.95–7.22 (m, 2H, 2CH_{Ar}). ¹³C NMR (CDCl₃) δ 22.8, 24.7, 25.0, 25.7, 26.7, 29.0, 45.4, 46.0, 49.4, 51.9, 54.0 (11CH₂), 59.2, 74.7, 116.9, 120.4 (4CH), 122.1 (C), 127.4, 129.7 (2CH), 154.6 (C), 163.4, 167.4 (2CO). Anal. (C₂₁H₂₉N₃O₃·HCl·2H₂O) C, H, N.

2-[4-[(3,4-Dihydro-2H-chromen-2-ylmethyl)amino]butyl]tetrahydro-2H-pyrrolo[1,2-a]pyra-zine-1,4(3H,6H)-dione (20). Obtained from 45 and amine 64 in 35% yield. Chromatography: EtOAc.

6-[4-[(3,4-Dihydro-2H-chromen-2-ylmethyl)amino]butyl]dihydroimidazo[5,1-b][1,3]thiazole-5,7(6H,7aH)-dione (21). Obtained from 46 and amine 64 in 43% yield. Chromatography: toluene/EtOH, 95:5; mp 149–151 °C (EtOAc). R_f (EtOAc/EtOH, 9:1) 0.17. IR (CHCl₃) ν 3400, 1770, 1718. ¹H NMR (CDCl₃) δ 1.48–1.86 (m, 5H, (CH₂)₂, 1/2CH₂_{chrom}), 2.01–2.10 (m, 1H, 1/2CH₂_{chrom}), 2.59–3.18 (m, 9H, 2CH₂NH, CH₂_{chrom}, 3/2CH₂_{cyo}), 3.53 (t, J = 7.0, 2H, CH₂N), 3.95–4.27 (s, 1H, CH), 4.49 (dd, J = 12.0, 6.0, 1H, 1/2CH₂_{cyo}), 5.08 (s, 1H, CHS), 6.56–6.92 (m, 2H, 2CH_{Ar}), 7.03–7.13 (m, 2H, 2CH_{Ar}). ¹³C NMR (CDCl₃) δ 23.9, 24.4, 25.5, 25.9, 32.7, 39.1, 48.4, 54.0, 58.3 (9CH₂), 63.2, 74.8, 116.7, 120.0 (4CH), 122.0 (C), 127.1, 129.4 (2CH), 154.6 (C), 159.6, 171.6 (2CO). Anal. (C₁₉H₂₅N₃O₃S·HCl) C, H, N.

6-[4-[(3,4-Dihydro-2H-chromen-2-ylmethyl)amino]butyl]-1H-imidazo[1,5-c][1,3]thiazole-5,7(6H,7aH)-dione (22). Obtained from 47 and amine 64 in 38% yield. Chromatography: toluene/EtOH, 95:5.

3-[4-[(3,4-Dihydro-2H-chromen-2-ylmethyl)amino]butyl]-1,3-thiazolidine-2,4-dione (23). Obtained from 48 and amine 64 in 45% yield. Chromatography: toluene/EtOH, 95:5; mp 126–127 °C (EtOAc). R_f (EtOAc) 0.21. IR (CHCl₃) ν 3400, 1750, 1683. ¹H NMR (CDCl₃) δ 1.47–1.76 (m, 5H, (CH₂)₂, 1/2CH₂_{chrom}), 2.01–2.06 (m, 1H, 1/2CH₂_{chrom}), 2.57–3.01 (m, 6H, 2CH₂NH, CH₂_{chrom}), 3.62 (t, J = 7.2, 2H, CH₂N), 3.92 (s, 2H, CH₂S), 4.10–4.25 (m, 1H, CH_{chrom}), 6.74–6.83 (m, 2H, 2CH_{Ar}), 7.01–7.08 (m, 2H, 2CH_{Ar}). ¹³C NMR (CDCl₃) δ 24.2, 24.5, 25.3, 25.9, 33.7, 41.8, 54.2, 58.4 (8CH₂), 74.3, 116.7, 120.0 (3CH), 122.0 (C), 127.1, 129.5 (2CH), 154.5 (C), 171.4, 171.8 (2CO). Anal. (C₁₇H₂₂N₂O₃S·HCl) C, H, N.

2-[3-[(3,4-Dihydro-2H-chromen-2-ylmethyl)amino]propyl]tetrahydro-1H-pyrrolo[1,2-c]imidazole-1,3(2H)-dione (24). Obtained from 49 and amine 64 in 40% yield. Chromatography: EtOAc.

2-[5-[(3,4-Dihydro-2H-chromen-2-ylmethyl)amino]pentyl]tetrahydro-1H-pyrrolo[1,2-c]imidazole-1,3(2H)-dione (25). Obtained from 50 and amine 64 in 50% yield. Chromatography: EtOAc/EtOH, 9:1.

2-[6-[(3,4-Dihydro-2H-chromen-2-ylmethyl)amino]hexyl]tetrahydro-1H-pyrrolo[1,2-c]imidazole-1,3(2H)-dione (26). Obtained from 51 and amine 64 in 35% yield. Chromatography: EtOAc/EtOH, 9:1.

2-[8-[(3,4-Dihydro-2H-chromen-2-ylmethyl)amino]octyl]tetrahydro-1H-pyrrolo[1,2-c]imidazole-1,3(2H)-dione (27). Obtained from 52 and amine 64 in 35% yield. Chromatography: EtOAc/EtOH, 95:5.

2-[(2E)-4-[(3,4-Dihydro-2H-chromen-2-ylmethyl)amino]but-2-enyl]tetrahydro-1H-pyrrolo[1,2-c]imidazole-1,3(2H)-dione (28). Obtained from 53 and amine 64 in 36% yield. Chromatography: EtOAc/EtOH, 9:1; oil. R_f (EtOAc/EtOH, 9:1) 0.30. IR (CHCl₃) ν 3375, 1771, 1709. ¹H NMR (CDCl₃) δ 1.63–2.31 (m, 6H, 2CH₂_{cyo}, CH₂_{chrom}), 2.65–2.93 (m, 4H, CH₂NH, CH₂_{chrom}), 3.17–3.31 (m, 3H, CH₂NH, 1/2CH₂_{cyo}), 3.67 (dt, J = 11.2, 7.6, 1H, 1/2CH₂_{cyo}), 4.03–

4.14 (m, 4H, CH₂N, CH_{cyo}, CH_{chrom}), 5.54–5.85 (m, 2H, CH=CH), 6.77–6.85 (m, 2H, 2CH_{Ar}), 7.00–7.10 (m, 2H, 2CH_{Ar}). ¹³C NMR (CDCl₃) δ 24.7, 25.7, 27.1, 27.6, 40.2, 45.6, 50.9, 53.6 (8CH₂), 63.5, 75.1, 116.8, 120.3 (4CH), 122.1 (C), 124.8, 127.3, 129.6, 132.3 (4CH), 154.6 (C), 160.4, 173.6 (2CO). Anal. (C₂₀H₂₅N₃O₃·HCl·4H₂O) C, H, N.

2-[(2Z)-4-[(3,4-Dihydro-2H-chromen-2-ylmethyl)amino]but-2-enyl]tetrahydro-1H-pyrrolo[1,2-c]imidazole-1,3(2H)-dione (29). Obtained from 54 and amine 64 in 38% yield. Chromatography: EtOAc.

2-[4-[(3,4-Dihydro-2H-chromen-2-ylmethyl)amino]but-2-ynyl]tetrahydro-1H-pyrrolo[1,2-c]imidazole-1,3(2H)-dione (30). Obtained from 55 and amine 64 in 36% yield. Chromatography: EtOAc.

2-[4-[(3,4-Dihydro-2H-chromen-2-ylmethyl)amino]methyl]benzyl]tetrahydro-1H-pyrrolo[1,2-c]imidazole-1,3(2H)-dione (31). Obtained from 56 and amine 64 in 35% yield. Chromatography: EtOAc; oil. R_f (EtOAc) 0.32. IR (CHCl₃) ν 3418, 1773, 1711. ¹H NMR (CDCl₃) δ 1.57–2.29 (m, 6H, 2CH₂_{cyo}, CH₂_{chrom}), 2.75–2.95 (m, 4H, CH₂NH, CH₂_{chrom}), 3.24 (ddd, J = 11.4, 7.3, 5.4, 1H, 1/2CH₂_{cyo}), 3.69 (dt, J = 11.2, 7.6, 1H, 1/2CH₂_{cyo}), 3.84 (s, 2H, ArCH₂NH), 4.04–4.22 (m, 2H, CH_{cyo}, CH_{chrom}), 4.61 (s, 2H, CH₂N), 6.82 (t, J = 8.1, 2H, 2CH_{Ar}), 7.01–7.11 (m, 2H, 2CH_{Ar}), 7.28–7.38 (m, 4H, 4CH_{Ar}). ¹³C NMR (CDCl₃) δ 24.5, 25.5, 26.8, 27.3, 42.1, 45.3 (6CH₂), 53.4 (2CH₂), 63.3, 75.1, 116.6, 120.0 (4CH), 121.6 (C), 127.0 (CH), 128.3 (2CH), 128.5 (2CH), 129.4 (CH), 134.3, 138.7 (2C), 155.8 (C), 156.1, 172.4 (2CO). Anal. (C₂₄H₂₇N₃O₃·HCl·2H₂O) C, H, N.

2-[3-[(3,4-Dihydro-2H-chromen-2-ylmethyl)amino]methyl]benzyl]tetrahydro-1H-pyrrolo[1,2-c]imidazole-1,3(2H)-dione (32). Obtained from 57 and amine 64 in 35% yield. Chromatography: EtOAc.

3-[5-[(3,4-Dihydro-2H-chromen-2-ylmethyl)amino]pentyl]-1,3-thiazolidine-2,4-dione (33). Obtained from 58 and amine 64 in 38% yield. Chromatography: toluene/EtOH, 20:1 to 8:2.

3-[6-[(3,4-Dihydro-2H-chromen-2-ylmethyl)amino]hexyl]-1,3-thiazolidine-2,4-dione (34). Obtained from 59 and amine 64 in 49% yield. Chromatography: EtOAc/EtOH, 9:1; oil. R_f (EtOAc/EtOH, 9:1) 0.20. IR (CHCl₃) ν 3416, 1751, 1670. ¹H NMR (CDCl₃) δ 1.25–2.01 (m, 10H, (CH₂)₄, CH₂_{chrom}), 2.66 (t, J = 7.1, 2H, CH₂NH), 2.76–2.95 (m, 4H, CH₂NH, CH₂_{chrom}), 3.62 (t, J = 7.3, 2H, CH₂N), 3.93 (s, 2H, CH₂S), 4.09–4.19 (m, 1H, CH_{chrom}), 6.78–6.85 (m, 2H, 2CH_{Ar}), 7.01–7.11 (m, 2H, 2CH_{Ar}). ¹³C NMR (CDCl₃) δ 24.6, 25.7, 26.6, 26.8, 27.5, 29.8, 33.7, 42.0, 49.8, 54.2 (10CH₂), 75.1, 116.7, 120.2 (3CH), 122.0 (C), 127.2, 129.5 (2CH), 154.6 (C), 171.4, 171.7 (2CO). Anal. (C₁₉H₂₆N₂O₃S·HCl) C, H, N.

3-[8-[(3,4-Dihydro-2H-chromen-2-ylmethyl)amino]octyl]-1,3-thiazolidine-2,4-dione (35). Obtained from 60 and amine 64 in 58% yield. Chromatography: EtOAc/EtOH, 9:1.

Binding Assays. For all receptors binding assays, male Sprague–Dawley rats (*Rattus norvegicus albinus*) weighing 180–200 g were killed by decapitation, and the brains were rapidly removed and dissected. Tissues were stored at –80 °C for subsequent use and homogenized on a Polytron PT-10 homogenizer. Membrane suspensions were centrifuged on a Beckman J2-HS instrument.

5-HT_{1A} Receptor. Binding assays were performed by a modification of the procedure previously described by Clark et al.⁶⁰ The cerebral cortex was homogenized in 10 volumes of ice-cold Tris buffer (50 mM Tris-HCl, pH 7.7 at 25 °C) and centrifuged at 28000g for 15 min. The membrane pellet was washed twice by resuspension and centrifugation. After the second wash the resuspended pellet was incubated at 37 °C for 10 min. Membranes were then collected by centrifugation, and the final pellet was resuspended in 50 mM Tris-HCl, 5 mM MgSO₄, and 0.5 mM EDTA buffer (pH 7.4 at 37 °C). Fractions of 100 μ L of the final membrane suspension (about 5 mg/mL of protein) were incubated at 37 °C for 15 min with 0.6 nM [³H]-8-OH-DPAT, in the presence or absence of the competing drug, in a final volume of 1.1 mL of assay buffer (50 mM Tris-HCl, 10 mM clonidine, 30 mM prazosin, pH 7.4 at 37 °C). Nonspecific binding was determined with 10 μ M 5-HT and represented less than 10% of total binding.

5-HT_{2A} Receptor. Binding assays were performed by a modification of the procedure previously described by Titeler et al.⁶¹ The frontal cortex was homogenized in 60 volumes of ice-cold buffer (50 mM Tris-HCl, 0.5 mM Na₂EDTA, 10 mM MgSO₄, pH 7.4 at 25 °C) and centrifuged at 30000g for 15 min at 4 °C. The membrane pellet was washed by resuspension and centrifugation. After the second wash, the resuspended pellet was incubated at 37 °C for 10 min. Membranes were then collected by centrifugation, and the final pellet was resuspended in 10 volumes of assay buffer (50 mM Tris-HCl, 0.5 mM Na₂EDTA, 10 mM MgSO₄, 0.1% ascorbic acid, 10 μM pargyline, pH 7.4 at 25 °C). Fractions of 100 μL of the final membrane suspension (about 5 mg/mL of protein) were incubated at 37 °C for 15 min with 0.4 nM [³H]ketanserin, in the presence or absence of the competing drug, in a final volume of 2 mL of assay buffer. Nonspecific binding was determined with 1 μM cinanserin and represented less than 15% of total binding.

5-HT₃ Receptor. Binding assays were performed by a modification of the procedure previously described by Wong et al.⁶² The cerebral cortex was homogenized in 9 volumes of ice-cold 0.32 M sucrose and centrifuged at 1000g for 10 min at 4 °C. The supernatant was centrifuged at 17000g for 20 min at 4 °C. The membrane pellet was washed twice by resuspension in 60 volumes of ice-cold 50 mM Tris-HCl buffer (pH 7.4 at 25 °C) and centrifugation at 48000g for 10 min at 4 °C. After the second wash, the resuspended pellet was incubated at 37 °C for 10 min and centrifuged at 48000g for 10 min at 4 °C. Membranes were resuspended in 2.75 volumes of assay buffer (50 mM Tris-HCl, 10 μM pargyline, 0.6 mM ascorbic acid, and 5 mM CaCl₂, pH 7.4 at 25 °C). Fractions of 100 μL of the final membrane suspension (about 2 mg/mL of protein) were incubated at 25 °C for 30 min with 0.7 nM [³H]LY 278584, in the presence or absence of the competing drug, in a final volume of 2 mL of assay buffer. Nonspecific binding was determined with 10 μM 5-HT and represented less than 20% of total binding.

5-HT₄ Receptor. Binding assays were performed by a modification of the procedure previously described by Grossman et al.⁶³ The striatum was homogenized in 15 volumes of ice-cold 50 mM HEPES buffer (pH 7.4 at 4 °C) and centrifuged at 48000g for 10 min. The pellet was resuspended in 20 volumes of assay buffer (50 mM HEPES, pH 7.4 at 25 °C). Fractions of 100 μL (about 5 mg/mL of protein) of the final membrane suspension were incubated at 37 °C for 30 min with 0.1 nM [³H]GR 113808, in the presence or absence of the competing drug, in a final volume of 1 mL of assay buffer. Nonspecific binding was determined with 30 μM 5-HT and represented less than 20% of total binding.

5-HT₇ Receptor. Binding assays were performed by a modification of the procedure previously described by Aguirre et al.⁶⁴ The hypothalamus was homogenized in 5 mL of ice-cold Tris buffer (50 mM Tris-HCl, pH 7.4 at 25 °C) and centrifuged at 48000g for 10 min. The membrane pellet was washed by resuspension and centrifugation, and then the resuspended pellet was incubated at 37 °C for 10 min. Membranes were then collected by centrifugation, and the final pellet was resuspended in 100 volumes of ice-cold assay buffer (50 mM Tris-HCl, 4 mM CaCl₂, 1 mg/mL ascorbic acid, 0.01 mM pargyline, and 3 μM pindolol⁶⁵ buffer (pH 7.4 at 25 °C)). Fractions of 400 μL of the final membrane suspension were incubated at 23 °C for 120 min with 0.5 nM [³H]-5-CT, in the presence or absence of the competing drug, in a final volume of 0.5 mL of assay buffer. Nonspecific binding was determined with 10 μM 5-HT and represented less than 15% of total binding.

D₂ Receptor. Binding assays were performed by a modification of the procedure previously described by Leysen et al.⁶⁶ The striatum was homogenized in 50 mM Tris-HCl (pH 7.4 at 25 °C) and centrifuged at 48000g for 10 min. The pellet was resuspended and centrifuged twice as before. The final pellet was resuspended in 20 volumes of assay buffer (50 mM Tris-HCl (pH 7.1 at 25 °C) containing 120 mM NaCl, 5 mM KCl, 1 mM CaCl₂, 1 mM MgCl₂, and 5.7 mM ascorbic acid). Fractions of the final membrane suspension (125–150 μg of protein) were incubated at 37 °C for 15 min with 0.11 nM [³H]spiperone, in the presence or absence of six concentrations of the competing drug, in a final volume of 0.55 mL of the assay buffer (pH

7.4 at 25 °C). Nonspecific binding was determined with 1 μM (+)-butaclamol and represented less than 20% of total binding.

α₁ Adrenoceptor. Binding assays were performed by a modification of the procedure previously described by Ambrosio et al.⁶⁷ The cerebral cortex was homogenized in 20 volumes of ice-cold buffer (50 mM Tris-HCl, 10 mM MgCl₂, pH 7.4 at 25 °C) and centrifuged at 30000g for 15 min. The pellet was washed twice by resuspension and centrifugation. The final pellet was resuspended in 20 volumes of the assay buffer. Fractions of the final membrane suspension (about 250 μg of protein) were incubated at 25 °C for 30 min with 0.2 nM [³H]prazosin, in the presence or absence of six concentrations of the competing drug, in a final volume of 2 mL of the assay buffer. Nonspecific binding was determined with 10 μM phentolamine and represented less than 20% of total binding.

8-OH-DPAT-Induced Hypothermia in Mice. The procedures used for these studies were based on previously described methods.⁶⁸ Briefly, male Swiss mice (23–28 g) were housed in groups of five, and body temperature was measured with a lubricated digital thermometer probe (pb0331, Panlab, Barcelona) inserted to a depth of 2 cm into the rectum of the mice. Temperature was recorded at 15, 30, and 60 min, after injection of 8-OH-DPAT or the compound to be tested. To study the antagonism to 8-OH-DPAT-induced hypothermia, compounds or vehicle (control) were administered intraperitoneally (ip) 30 min before the injection of 8-OH-DPAT (0.5 mg/kg, subcutaneously). The hypothermic response to 8-OH-DPAT was measured as the maximum decrease in body temperature recorded in this period. The results were expressed as change in body temperature with respect to basal temperature, measured at the beginning of the experiment. The obtained data were analyzed by Anova followed by Student–Newman–Keuls test.

cAMP Formation in HeLa Cells Transfected with the h5-HT_{1AR}.⁶⁹ A HeLa cell line permanently expressing the h5-HT_{1AR} gene (kindly donated by Cajal Institute, Madrid) was cultured in Dulbecco's modified Eagle medium (DMEM) supplemented with 2 mM glutamine, 1 mM pyruvate, and 10% heat-inactivated fetal calf serum (FCS). Subcultures were made by using 0.025% trypsin in phosphate buffered saline (PBS). Cultures were maintained at 37 °C in an air/CO₂ (95:5) water-saturated atmosphere. cAMP experiments were carried out with cultures grown for 2–3 days in 8-well culture plates with 2 mL medium/well.

Cultures (about 7.5 × 10⁴ cells/well) were washed with PBS and incubated for 10 min with 1 mL of PBS containing 0.5 mM isobutylmethylxanthine and 10 μM forskolin in the presence or absence of test compounds. The medium was then aspirated, and the reaction stopped by addition of 600 μL of ice-cold ethanol. Two hours later, ethanol was taken into an Eppendorf tube to be lyophilized, and the resulting pellet was resuspended in 100 μL of assay buffer (Kit Amersham SPA, RPA 538) and cAMP was quantified by RIA. To study the antagonism to 8-OH-DPAT-induced inhibition of forskolin-induced cAMP formation, test compounds were preincubated 20 min before the addition of forskolin and 8-OH-DPAT.

Neurotoxicity Assays in Cell Cultures. Primary neuronal cultures were prepared from hippocampi of fetal Wistar rats at embryonic day 18 (E18). After dissection and mechanical dissociation, cells were cultured on poly-L-lysine coated plates at 37 °C in a humidified 5% CO₂ atmosphere. Two types of cell cultures were prepared. For mixed neuronal and glial cells cultures, cells were maintained in Neurobasal medium (Invitrogen) containing 0.5 mM glutamine, 100 U/mL penicillin, and 100 μg/mL streptomycin and supplemented with 10% FCS. For the preparation of neuronal cell-enriched cultures, FCS was substituted by 2% B27 supplement (Invitrogen).

Neurotoxicity studies were performed after 11 days in vitro. To determine the protection against apoptotic cell death induced by serum deprivation, culture medium was replaced by saline in mixed cultures, and cells were incubated in the presence of test compounds for 24 h. To study the protection against glutamate toxicity, 1 mM glutamate was added to neuron-enriched cultures for 22 h, and different concentrations of test compounds (1 nM to 10 μM) were added 30 min before glutamate. Exposure to oxygen and glucose

deprivation in neuron-enriched cultures was performed as described.⁷⁰ Culture medium was replaced by a solution containing (mM): 130 NaCl, 5.4 KCl, 1.8 CaCl₂, 26 NaHCO₃, 0.8 MgSO₄, 1.18 NaH₂PO₄, and 25 2-desoxy-D-glucose. Cells were transferred to an anaerobic chamber (Forma Scientific, Hucoer-Erloss) containing 95% N₂/5% CO₂ at 37 °C for 150 min. After this time, the solution was replaced by DMEM medium supplemented with 33 mM glucose, and plates were incubated for 18 h in 5% CO₂ atmosphere. Test compounds were added at the time of initiating oxygen-glucose deprivation. Cell survival was estimated by measuring the activity of mitochondrial dehydrogenase on 3-(4,5-dimethylthiazol-2-yl)-2,5-diphenyltetrazolium bromide (MTT), as described.⁷¹

Focal Cerebral Ischemia in Rats. Focal cerebral ischemia was produced in male Sprague–Dawley rats by permanent intraluminal MCAO, as previously reported.^{72,73} The day before ischemia, anesthesia was induced with 4% halothane. Rats were placed in the prone position on a stereotaxic frame, and anesthesia was maintained with 1.5–2% halothane. The left femoral artery was cannulated to monitor mean arterial blood pressure, and body temperature was maintained at 37.5 °C with a heating blanket connected to a rectal probe. A 2.6 cm length of 3–0 monofilament nylon suture heat-blunted at the tip was introduced into the external carotid artery through a puncture. The nylon suture was gently advanced into the internal carotid artery and circle of Willis until the origin of the MCA was reached, at approximately 22 mm from the carotid bifurcation. Infarct volume was measured 24 h later. Rats were killed while under halothane anesthesia, and the brains were rapidly frozen and kept at –20 °C. Coronal brain sections of 20 μm were obtained with a cryostat and stained with a 1% solution of the mitochondrial dye TTC for 10 min. The infarcted area was identified macroscopically by pallor and microscopically by structural disorganization and histologic signs of neuronal and tissular damage. Infarct area was measured in each stained section with an image analyzing system (AIM Image Research). Test compounds were iv administered (intravenously bolus injection) one hour before ischemia and one hour later or, alternatively, were given by continuous iv infusion.

Molecular Modeling. Modeler v9.5⁷⁴ was used to build a homology model of the human 5-HT_{1A}R using the crystal structure of the β₂-adrenergic receptor (PDB code 2RH1)⁴⁶ as template. The general Amber force field (GAFF) and HF/6-31G*-derived RESP atomic charges were used for the ligand. Molecular dynamics simulation of the ligand–receptor complex were performed with the Sander module of AMBER 10⁷⁵ using the protocol previously described.⁷⁶

■ ASSOCIATED CONTENT

Supporting Information

Spectral characterization data of compounds 5–7, 10, 11, 13–15, 17, 18, 20, 22, 24–27, 29, 30, 32, 33, 35, 47, 48, 50–52, 54, and 57–60 as well as combustion analysis data of final compounds 4–35. This material is available free of charge via the Internet at <http://pubs.acs.org>.

■ AUTHOR INFORMATION

Corresponding Author

*For M.L.L.-R.: phone, 34-91-3944239; fax, 34-91-3944103; E-mail, mluzlr@quim.ucm.es. For B.B.: phone, 34-91-3945156; fax, 34-91-3944103; E-mail, bellinda.benhamu@quim.ucm.es.

Author Contributions

[#]These authors contributed equally to this work.

■ ACKNOWLEDGMENTS

This work was supported by grants from MICINN (SAF2008-02342 and SAF2010-22198), CAM (S-SAL-249-2006), FIMA (UTE project), and ISCIII (RD07/0067/0008). We thank the NMR Core Facilities from Universidad Complutense de Madrid.

■ ABBREVIATIONS USED

DMEM, Dulbecco's modified Eagle medium; FCS, fetal calf serum; GPCR, G protein-coupled receptor; h5-HT_{1A}R, human 5-HT_{1A} receptor; ip, intraperitoneally; iv, intravenously; MCAO, occlusion of the middle cerebral artery; PBS, phosphate buffered saline; TM, transmembrane

■ REFERENCES

- (1) Filmore, D. It's a GPCR world. *Modern Drug Discovery* **2004**, *7*, 24–28.
- (2) Lagerstrom, M. C.; Schioth, H. B. Structural diversity of G protein-coupled receptors and significance for drug discovery. *Nature Rev. Drug Discovery* **2008**, *7*, 339–357.
- (3) Rosenbaum, D. M.; Rasmussen, S. G. F.; Kobilka, B. K. The structure and function of G-protein-coupled receptors. *Nature* **2009**, *459*, 356–363.
- (4) Congreve, M.; Marshall, F. The impact of GPCR structures on pharmacology and structure-based drug design. *Br. J. Pharmacol.* **2010**, *159*, 986–996.
- (5) Hoyer, D.; Martin, G. 5-HT receptor classification and nomenclature: towards a harmonization with the human genome. *Neuropharmacology* **1997**, *36*, 419–428.
- (6) Nichols, D. E.; Nichols, C. D. Serotonin receptors. *Chem. Rev.* **2008**, *108*, 1614–1641.
- (7) Schreiber, R.; Devry, J. 5-HT(1A) Receptor ligands in animal-models of anxiety, impulsivity and depression—multiple mechanisms of action. *Prog. Neuro-Psychopharmacol. Biol. Psychiatry* **1993**, *17*, 87–104.
- (8) Blier, P.; Ward, N. M. Is there a role for 5-HT_{1A} agonists in the treatment of depression? *Biol. Psychiatry* **2003**, *53*, 193–203.
- (9) Savitz, J.; Lucki, I.; Drevets, W. C. 5-HT_{1A} receptor function in major depressive disorder. *Prog. Neurobiol.* **2009**, *88*, 17–31.
- (10) Bantick, R. A.; Deakin, J. F. W.; Grasby, P. M. The 5-HT_{1A} receptor in schizophrenia: a promising target for novel atypical neuroleptics? *J. Psychopharmacol.* **2001**, *15*, 37–46.
- (11) McCreary, A. C.; Jones, C. A. Antipsychotic medication: the potential role of 5-HT_{1A} receptor agonism. *Curr. Pharm. Des.* **2010**, *16*, 516–521.
- (12) Bara-Jimenez, W.; Bibbiani, F.; Morris, M. J.; Dimitrova, T.; Sherzai, A.; Mouradian, M. M.; Chase, T. N. Effects of serotonin 5-HT_{1A} agonist in advanced Parkinson's disease. *Mov. Dis.* **2005**, *20*, 932–936.
- (13) Mico, J. A.; Berrocoso, E.; Ortega-Alvaro, A.; Gibert-Rahola, J.; Rojas-Corrales, M. O. The role of 5-HT_{1A} receptors in research strategy for extensive pain treatment. *Curr. Top. Med. Chem.* **2006**, *6*, 1997–2003.
- (14) Ogren, S. O.; Eriksson, T. M.; Elvander-Tottie, E.; D'Addario, C.; Ekstrom, J. C.; Svenningsson, P.; Meister, B.; Kehr, J.; Stiedl, O. The role of 5-HT_{1A} receptors in learning and memory. *Behav. Brain Res.* **2008**, *195*, 54–77.
- (15) Lacivita, E.; Leopoldo, M.; Berardi, F.; Perrone, R. 5-HT_{1A} receptor, an old target for new therapeutic agents. *Curr. Top. Med. Chem.* **2008**, *8*, 1024–1034.
- (16) Madhavan, L.; Freed, W. J.; Anantharam, V.; Kanthasamy, A. G. 5-Hydroxytryptamine 1A receptor activation protects against N-methyl-D-aspartate-induced apoptotic cell death in striatal and mesencephalic cultures. *J. Pharmacol. Exp. Ther.* **2003**, *304*, 913–923.
- (17) Chang, C. P.; Chen, S. H.; Lin, M. T. Ipsapirone and ketanserin protects against circulatory shock, intracranial hypertension, and cerebral ischemia during heatstroke. *Shock* **2005**, *24*, 336–340.
- (18) Kamei, K.; Maeda, N.; Nomura, K.; Shibata, M.; Katsuragi-Ogino, R.; Koyama, M.; Nakajima, M.; Inoue, T.; Ohno, T.; Tatsuoka, T. Synthesis, SAR studies, and evaluation of 1,4-benzoxazepine derivatives as selective 5-HT_{1A} receptor agonists with neuroprotective effect: discovery of Piclozotan. *Bioorg. Med. Chem.* **2006**, *14*, 1978–1992.
- (19) Berends, A. C.; Luiten, P. G.; Nyakas, C. A review of the neuroprotective properties of the 5-HT_{1A} receptor agonist repinotan

HCl (BAYx3702) in ischemic stroke. *CNS Drug Rev.* **2005**, *11*, 379–402.

(20) Iannuzzi, N. P.; Liebeskind, D. S.; Jacoby, M.; Arima, K.; Shimizu, K.; Asubio, D.; Zimmerman, T. R. Piclozotan (SUN N4057), a novel 5-HT_{1A} receptor agonist, is well tolerated in patients with acute stroke. *Stroke* **2006**, *37*, 655–655.

(21) Teal, P.; Davis, S.; Hacke, W.; Kaste, M.; Lyden, P. D.; Fierus, M. A. Randomized, double-blind, placebo-controlled trial to evaluate the efficacy, safety, tolerability, and pharmacokinetic/pharmacodynamic effects of a targeted exposure of intravenous repinotan in patients with acute ischemic stroke modified randomized exposure controlled trial. *Stroke* **2009**, *40*, 3518–3525.

(22) Kuzumaki, O.; Narita, M.; Suzuki, T. Effect of the stimulation of serotonin(1A) (5-HT_{1A}) receptor on neurogenesis and neuroprotection. *J. Pharmacol. Sci.* **2006**, *101*, 116.

(23) Salazar-Colocho, P.; Del Rio, J.; Frechilla, D. Serotonin 5-HT_{1A} receptor activation prevents phosphorylation of NMDA receptor NR1 subunit in cerebral ischemia. *J. Physiol. Biochem.* **2007**, *63*, 203–211.

(24) Salazar-Colocho, P.; Del Rio, J.; Frechilla, D. Neuroprotective effects of serotonin 5-HT_{1A} receptor activation against ischemic cell damage in gerbil hippocampus: involvement of NMDA receptor NR1 subunit and BDNF. *Brain Res.* **2008**, *1199*, 159–166.

(25) Lopez-Rodriguez, M. L.; Rosado, M. L.; Benhamu, B.; Morcillo, M. J.; Sanz, A. M.; Orensanz, L.; Beneitez, M. E.; Fuentes, J. A.; Manzanara, J. Synthesis and structure–activity relationships of a new model of arylpiperazines. 1. 2-[[4-(*o*-Methoxyphenyl)piperazin-1-yl]methyl]-1,3-dioxoperhydroimidazo[1,5-*a*]pyridine: a selective 5-HT_{1A} receptor agonist. *J. Med. Chem.* **1996**, *39*, 4439–4450.

(26) Lopez-Rodriguez, M. L.; Morcillo, M. J.; Fernández, E.; Porras, E.; Murcia, M.; Sanz, A. M.; Orensanz, L. Synthesis and structure–activity relationships of a new model of arylpiperazines. 3. 2-[Omega-(4-arylpiperazin-1-yl)alkyl]perhydropyrrolo[1,2-*c*]imidazoles and -perhydroimidazo[1,5-*a*]pyridines: study of the influence of the terminal amide fragment on 5-HT_{1A} affinity/selectivity. *J. Med. Chem.* **1997**, *40*, 2653–2656.

(27) Lopez-Rodriguez, M. L.; Morcillo, M. J.; Fernandez, E.; Porras, E.; Orensanz, L.; Beneytez, M. E.; Manzanara, J.; Fuentes, J. A. Synthesis and structure–activity relationships of a new model of arylpiperazines. 5. Study of the physicochemical influence of the pharmacophore on 5-HT_{1A}/alpha(1)-adrenergic receptor affinity: synthesis of a new derivative with mixed 5-HT_{1A}/D₂ antagonist properties. *J. Med. Chem.* **2001**, *44*, 186–197.

(28) Lopez-Rodriguez, M. L.; Morcillo, M. J.; Fernandez, E.; Rosado, M. L.; Pardo, L.; Schaper, K. J. Synthesis and structure–activity relationships of a new model of arylpiperazines. 6. Study of the 5-HT_{1A}/alpha(1)-adrenergic receptor affinity by classical Hansch analysis, artificial neural networks, and computational simulation of ligand recognition. *J. Med. Chem.* **2001**, *44*, 198–207.

(29) Lopez-Rodriguez, M. L.; Ayala, D.; Benhamu, B.; Morcillo, M. J.; Viso, A. Arylpiperazine derivatives acting at 5-HT_{1A} receptors. *Curr. Med. Chem.* **2002**, *9*, 443–469.

(30) Lopez-Rodriguez, M. L.; Ayala, D.; Viso, A.; Benhamu, B.; de la Pradilla, R. F.; Zarza, F.; Ramos, J. A. Synthesis and structure–activity relationships of a new model of arylpiperazines. Part 7: Study of the influence of lipophilic factors at the terminal amide fragment on 5-HT_{1A} affinity/selectivity. *Bioorg. Med. Chem.* **2004**, *12*, 1551–1557.

(31) Lopez-Rodriguez, M. L.; Morcillo, M. J.; Fernandez, E.; Benhamu, B.; Tejada, I.; Ayala, D.; Viso, A.; Campillo, M.; Pardo, L.; Delgado, M.; Manzanara, J.; Fuentes, J. A. Synthesis and structure–activity relationships of a new model of arylpiperazines. 8. Computational simulation of ligand–receptor interaction of 5-HT_{1A}R agonists with selectivity over alpha1-adrenoceptors. *J. Med. Chem.* **2005**, *48*, 2548–2558.

(32) Caicoya, A. G.; Beneytez, M. L.; Delgado, M.; Manzanara, J.; Lopez-Rodriguez, M. L.; Benhamu, B.; Morcillo, M. J.; Pozo, M. A.; Rubia, F. J.; Fuentes, J. A. Biochemical, electrophysiological and neurohormonal studies with B-20991, a selective 5-HT_{1A} receptor agonist. *Pharmacology* **2001**, *62*, 234–242.

(33) Delgado, M.; Caicoya, A. G.; Greciano, V.; Benhamu, B.; Lopez-Rodriguez, M. L.; Fernandez-Alfonso, M. S.; Pozo, M. A.; Manzanara, J.; Fuentes, J. A. Anxiolytic-like effect of a serotonergic ligand with high affinity for 5-HT_{1A}, 5-HT_{2A} and 5-HT₃ receptors. *Eur. J. Pharmacol.* **2005**, *511*, 9–19.

(34) Robertson, A. V.; Francis, J. E.; Witkop, B. Rearrangements of dehydroproline derivatives. *J. Am. Chem. Soc.* **1962**, *84*, 1709–1715.

(35) Freed, M. E.; Day, A. R. Syntheses of 1,4-diazabicyclo[4.4.0]decanes, 1,4-diazabicyclo[4.3.0]nonanes and 1,8-diazabicyclo[4.3.0]nonanes. *J. Org. Chem.* **1960**, *25*, 2108–2113.

(36) Armstrong, M. D. The hydantoin derivative of 4-thiazolidinecarboxylic acid. *J. Am. Chem. Soc.* **1955**, *77*, 6049–6049.

(37) Vicar, J.; Smolikov, J.; Blaha, K. Amino-acids and peptides. 2,5-Piperazinediones with an annealed azetidine ring—synthesis and infrared spectra. *Collect. Czech. Chem. Commun.* **1973**, *38*, 1957–1970.

(38) Kayser, K. J.; Glenn, M. P.; Sebt, S. M.; Cheng, J. Q.; Hamilton, A. D. Modifications of the GSK3 beta substrate sequence to produce substrate-mimetic inhibitors of Akt as potential anti-cancer therapeutics. *Bioorg. Med. Chem. Lett.* **2007**, *17*, 2068–2073.

(39) Zahn, S.; Canary, J. W. Cu(I/II) redox control of molecular conformation and shape in chiral tripodal ligands: Binary exciton-coupled circular dichroic states. *J. Am. Chem. Soc.* **2002**, *124*, 9204–9211.

(40) Maryanoff, B. E.; McComsey, D. F.; Costanzo, M. J.; Hochman, C.; Smith-Swintosky, V.; Shank, R. P. Comparison of sulfamate and sulfamide groups for the inhibition of carbonic anhydrase-II by using topiramate as a structural platform. *J. Med. Chem.* **2005**, *48*, 1941–1947.

(41) Kwalk, J. H.; Won, S. W.; Kim, T. J.; Roh, E.; Kang, H. Y.; Lee, H. W.; Jung, J. K.; Hwang, B. Y.; Kim, Y.; Cho, J.; Lee, H. Synthesis of chroman-2-carboxylic acid *N*-(substituted)phenylamides and their inhibitory effect on nuclear factor-kappa B (NF-kappa B) activation. *Arch. Pharm. Res.* **2008**, *31*, 133–141.

(42) Kalaritis, P.; Regenye, R. W.; Partridge, J. J.; Coffen, D. L. Kinetic resolution of 2-substituted esters catalyzed by a lipase ex *Pseudomonas fluorescens*. *J. Org. Chem.* **1990**, *55*, 812–815.

(43) Cheng, Y.; Prusoff, W. H. Relationship between the inhibition constant (K_i) and the concentration of inhibitor which causes 50% inhibition (I_{50}) of an enzymatic reaction. *Biochem. Pharmacol.* **1973**, *22*, 3099–3108.

(44) Warne, T.; Serrano-Vega, M. J.; Baker, J. G.; Moukhametzianov, R.; Edwards, P. C.; Leslie, A. G.; Tate, C. G.; Schertler, G. F. Structure of a beta1-adrenergic G-protein-coupled receptor. *Nature* **2008**, *454*, 486–491.

(45) Warne, T.; Moukhametzianov, R.; Baker, J. G.; Nehme, R.; Edwards, P. C.; Leslie, A. G. W.; Schertler, G. F. X.; Tate, C. G. The structural basis for agonist and partial agonist action on a beta(1)-adrenergic receptor. *Nature* **2011**, *469*, 241–244.

(46) Rosenbaum, D. M.; Cherezov, V.; Hanson, M. A.; Rasmussen, S. G.; Thian, F. S.; Kobilka, T. S.; Choi, H. J.; Yao, X. J.; Weis, W. I.; Stevens, R. C.; Kobilka, B. K. GPCR engineering yields high-resolution structural insights into beta2-adrenergic receptor function. *Science* **2007**, *318*, 1266–1273.

(47) Rasmussen, S. G.; Choi, H. J.; Fung, J. J.; Pardon, E.; Casarosa, P.; Chae, P. S.; Devree, B. T.; Rosenbaum, D. M.; Thian, F. S.; Kobilka, T. S.; Schnapp, A.; Konetzi, I.; Sunahara, R. K.; Gellman, S. H.; Pautsch, A.; Steyaert, J.; Weis, W. I.; Kobilka, B. K. Structure of a nanobody-stabilized active state of the beta(2) adrenoceptor. *Nature* **2011**, *469*, 175–180.

(48) Rosenbaum, D. M.; Zhang, C.; Lyons, J. A.; Holl, R.; Aragao, D.; Arlow, D. H.; Rasmussen, S. G.; Choi, H. J.; Devree, B. T.; Sunahara, R. K.; Chae, P. S.; Gellman, S. H.; Dror, R. O.; Shaw, D. E.; Weis, W. I.; Caffrey, M.; Gmeiner, P.; Kobilka, B. K. Structure and function of an irreversible agonist-beta(2) adrenoceptor complex. *Nature* **2011**, *469*, 236–240.

(49) Chien, E. Y.; Liu, W.; Zhao, Q.; Katritch, V.; Han, G. W.; Hanson, M. A.; Shi, L.; Newman, A. H.; Javitch, J. A.; Cherezov, V.; Stevens, R. C. Structure of the human dopamine D₃ receptor in

complex with a D₂/D₃ selective antagonist. *Science* **2010**, *330*, 1091–1095.

(50) Shimamura, T.; Shiroishi, M.; Weyand, S.; Tsujimoto, H.; Winter, G.; Katritch, V.; Abagyan, R.; Cherezov, V.; Liu, W.; Han, G. W.; Kobayashi, T.; Stevens, R. C.; Iwata, S. Structure of the human histamine H(1) receptor complex with doxepin. *Nature* **2011**, *475*, 65–70.

(51) Rosenkilde, M. M.; Benned-Jensen, T.; Frimurer, T. M.; Schwartz, T. W. The minor binding pocket: a major player in 7TM receptor activation. *Trends Pharmacol. Sci.* **2010**, *31*, 567–574.

(52) Gonzalez, A.; Murcia, M.; Benhamu, B.; Campillo, M.; Lopez-Rodriguez, M. L.; Pardo, L. The importance of solvation in the design of ligands targeting membrane proteins. *Med. Chem. Commun.* **2011**, *2*, 160–164.

(53) Oosterink, B. J.; Korte, S. M.; Nyakas, C.; Korf, J.; Luiten, P. G. M. Neuroprotection against N-methyl-D-aspartate-induced excitotoxicity in rat magnocellular nucleus basalis by the 5-HT_{1A} receptor agonist 8-OH-DPAT. *Eur. J. Pharmacol.* **1998**, *358*, 147–152.

(54) Suchanek, B.; Struppeck, H.; Fahrig, T. The 5-HT_{1A} receptor agonist BAY x 3702 prevents staurosporine-induced apoptosis. *Eur. J. Pharmacol.* **1998**, *355*, 95–101.

(55) Dakin, H. D. Amino acids of gelatin. *J. Biol. Chem.* **1920**, *44*, 499–529.

(56) Vicar, J.; Smolikova, J.; Blaha, K. Synthesis and infrared spectroscopy of 2,5-piperazinediones derived from proline and piperolic acid. *Collect. Czech. Chem. Commun.* **1972**, *37*, 4060–4071.

(57) Zhang, M.; Reeves, R.; Bi, C.; Dally, R.; Ladouceur, G.; Bullock, W.; Chin, J. Synthesis of optically active 6-substituted 2-(aminomethyl)chromans. *Tetrahedron Lett.* **2004**, *45*, 5229–5231.

(58) Urban, F. J.; Moore, B. S. Synthesis of optically active 2-benzylidihydrobenzopyrans for the hypoglycemic agent englitazone. *J. Heterocycl. Chem.* **1992**, *29*, 431–438.

(59) Junge, B.; Schohe, R.; Seidel, P.-R.; Glaser, T.; Traber, J.; Benz, U.; Schuurman, T.; De Vry, J.-M. V. Substituted aminomethyltetralins and their heterocyclic analogues. US Patent US5137901, 1992.

(60) Clark, R. D.; Weinhardt, K. K.; Berger, J.; Fisher, L. E.; Brown, C. M.; MacKinnon, A. C.; Kilpatrick, A. T.; Spedding, M. 1,9-Alkano-bridged 2,3,4,5-tetrahydro-1H-3-benzazepines with affinity for the alpha 2-adrenoceptor and the 5-HT_{1A} receptor. *J. Med. Chem.* **1990**, *33*, 633–641.

(61) Titeler, M.; Lyon, R. A.; Davis, K. H.; Glennon, R. A. Selectivity of serotonergic drugs for multiple brain serotonin receptors. Role of [³H]-4-bromo-2,5-dimethoxyphenylisopropylamine ([³H]DOB), a 5-HT₂ agonist radioligand. *Biochem. Pharmacol.* **1987**, *36*, 3265–3271.

(62) Wong, D. T.; Robertson, D. W.; Reid, L. R. Specific [³H]LY278584 binding to 5-HT₃ recognition sites in rat cerebral cortex. *Eur. J. Pharmacol.* **1989**, *166*, 107–110.

(63) Grossman, C. J.; Kilpatrick, G. J.; Bunce, K. T. Development of a radioligand binding assay for 5-HT₄ receptors in guinea-pig and rat brain. *Br. J. Pharmacol.* **1993**, *109*, 618–624.

(64) Aguirre, N.; Ballaz, S.; Lasheras, B.; Del Rio, J. MDMA (“Ecstasy”) enhances 5-HT_{1A} receptor density and 8-OH-DPAT-induced hypothermia: blockade by drugs preventing 5-hydroxytryptamine depletion. *Eur. J. Pharmacol.* **1998**, *346*, 181–188.

(65) Fone, K. C. F.; Marsden, C. A. Serotonin 5-HT₇ receptors binding to rat hypothalamic membranes—reply. *J. Neurochem.* **1999**, *72*, 883–884.

(66) Leysen, J. E.; Gommeren, W.; Laduron, P. M. Spiperone—ligand of choice for neuroleptic receptors 1. Kinetics and characteristics of in vitro binding. *Biochem. Pharmacol.* **1978**, *27*, 307–316.

(67) Ambrosio, E.; Montero, M. T.; Fernandez, I.; Azuara, M. C.; Orensanz, L. M. [³H]Prazosin binding to central nervous system regions of male and female rats. *Neurosci. Lett.* **1984**, *49*, 193–197.

(68) Bill, D. J.; Knight, M.; Forster, E. A.; Fletcher, A. Direct evidence for an important species difference in the mechanism of 8-OH-DPAT-induced hypothermia. *Br. J. Pharmacol.* **1991**, *103*, 1857–1864.

(69) Pauwels, P. J.; Van Gompel, P.; Leysen, J. E. Activity of serotonin (5-HT) receptor agonists, partial agonists and antagonists at

cloned human 5-HT_{1A} receptors that are negatively coupled to adenylate cyclase in permanently transfected HeLa cells. *Biochem. Pharmacol.* **1993**, *45*, 375–383.

(70) De Cristobal, J.; Cardenas, A.; Lizasoain, I.; Leza, J. C.; Fernandez-Tome, P.; Lorenzo, P.; Moro, M. A. Inhibition of glutamate release via recovery of ATP levels accounts for a neuroprotective effect of aspirin in rat cortical neurons exposed to oxygen-glucose deprivation. *Stroke* **2002**, *33*, 261–267.

(71) Hansen, M. B.; Nielsen, S. E.; Berg, K. Re-examination and further development of a precise and rapid dye method for measuring cell growth/cell kill. *J. Immunol. Methods* **1989**, *119*, 203–210.

(72) Planas, A. M.; Sole, S.; Justicia, C. Expression and activation of matrix metalloproteinase-2 and -9 in rat brain after transient focal cerebral ischemia. *Neurobiol. Dis.* **2001**, *8*, 834–846.

(73) Perez-Asensio, F. J.; de la Rosa, X.; Jimenez-Altayo, F.; Gorina, R.; Martinez, E.; Messeguer, A.; Vila, E.; Chamorro, A.; Planas, A. M. Antioxidant CR-6 protects against reperfusion injury after a transient episode of focal brain ischemia in rats. *J. Cereb. Blood. Flow Metab.* **2010**, *30*, 638–652.

(74) Marti-Renom, M. A.; Stuart, A. C.; Fiser, A.; Sanchez, R.; Melo, F.; Sali, A. Comparative protein structure modeling of genes and genomes. *Annu. Rev. Biophys. Biomol. Struct.* **2000**, *29*, 291–325.

(75) Case, D. A.; Darden, T. A.; Cheatham, T. E., III; Simmerling, C. L.; Wang, J.; Duke, R. E.; Luo, R.; Crowley, M.; Walker, R. C.; Zhang, W.; Merz, K. M.; Wang, B.; Hayik, S.; Roitberg, A.; Seabra, G.; Kolossvary, I.; Wong, K. F.; Paesani, F.; Vanicek, J.; Wu, X.; Brozell, S.; Steinbrecher, T.; Gohlke, H.; Yang, L.; Tan, C.; Mongan, J.; Hornak, V.; Cui, G.; Mathews, D. H.; Seetin, M. G.; Sagui, C.; Babin, V.; Kollman, P. A. *AMBER 10*; University of California: San Francisco, 2008.

(76) de la Fuente, T.; Martin-Fontecha, M.; Sallander, J.; Benhamu, B.; Campillo, M.; Medina, R. A.; Pellissier, L. P.; Claeysen, S.; Dumuis, A.; Pardo, L.; Lopez-Rodriguez, M. L. Benzimidazole derivatives as new serotonin 5-HT₆ receptor antagonists. Molecular mechanisms of receptor inactivation. *J. Med. Chem.* **2010**, *53*, 1357–1369.